1965

Static bending tests on longitudinally stiffened plate girders

Michael A. D'Apice
Lehigh University

STATIC BENDING TESTS ON LONGITUDINALLY STIFFENED PLATE GIRDERS

by
Michael A. D'Apice

ABSTRACT

This thesis describes static bending tests of five longitudinally stiffened plate girders. The experimental variables were the panel size and longitudinal stiffener size. The primary test objectives were: (1) to determine to what extent longitudinal stiffeners can contribute to the resistance of the web to vertical buckling of the compression flange, (2) to determine how the stress redistribution at loads above the theoretical web buckling load is affected by the presence of a longitudinal stiffener and (3) to determine to what extent lateral web deflections can be reduced by the use of a longitudinal stiffener.

The test setup and test procedure are described and the results are analyzed and discussed. It is concluded that the longitudinal stiffeners were effective in retarding stress redistribution and in controlling web deflections, but for the stiffener sizes used in these tests, no significant increase in bending strength due to the presence of longitudinal stiffeners was observed.

STATIC BENDING TESTS ON

LONGITUDINALLY STIFFENED PLATE GIRDERS

by

Michael A. D'Apice

A Thesis

Presented to the Graduate Faculty

of Lehigh University

in Candidacy for the Degree of

Master of Science

Lehigh University

1965

CERTIFICATE OF APPROVAL

This thesis is accepted and approved in partial fulfillment of the requirements for the degree of Master of Science in Civil Engineering.

April 29, 1965
(Date)

T. V. Galambos
Professor Theodore V. Galambos
Professor in Charge

C. P. Siess for
Professor William J. Eney, Head
Department of Civil Engineering

ACKNOWLEDGMENTS

The author wishes to thank Dr. Theodore V. Galambos, Professor in charge of the thesis, for his guidance during its preparation. He also wishes to express his deepest gratitude to Mr. Peter B. Cooper for his very invaluable assistance in the preparation of this report.

The work described in this thesis is part of an investigation on "Longitudinally Stiffened Plate Girders" being conducted under the direction of Dr. Theodore V. Galambos. Dr. Lynn S. Beedle is Director of Fritz Engineering Laboratory where the work was performed and Professor William J. Eney is Head of the Department of Civil Engineering and Fritz Engineering Laboratory. The project is sponsored by the Pennsylvania Department of Highways in conjunction with the U. S. Department of Commerce - Bureau of Public Roads and the American Iron and Steel Institute through the Welding Research Council.

The assistance of Messrs. Joseph A. Corrado and David J. Fielding in the actual testing program is appreciated as is the assistance of the laboratory technicians in preparing the test setups and that of the draftsmen in preparing the drawings.

TABLE OF CONTENTS

LIST OF TABLES

LIST OF FIGURES

LIST OF FIGURES (Cont'd)

ABSTRACT

This thesis describes static bending tests of five longitudinally stiffened plate girders. The experimental variables were the panel size and longitudinal stiffener size. The primary test objectives were: (1) to determine to what extent longitudinal stiffeners can contribute to the resistance of the web to vertical buckling of the compression flange, (2) to determine how the stress redistribution at loads above the theoretical web buckling load is affected by the presence of a longitudinal stiffener and (3) to determine to what extent lateral web deflections can be reduced by the use of a longitudinal stiffener.

The test setup and test procedure are described and the results are analyzed and discussed. It is concluded that the longitudinal stiffeners were effective in retarding stress redistribution and in controlling web deflections, but for the stiffener sizes used in these tests, no significant increase in bending strength due to the presence of longitudinal stiffeners was observed.

1. INTRODUCTION

Prior to 1961 the provisions for the design of steel plate girders in most specifications were based on the theoretical buckling strength of the web. Theoretical and experimental research on transversely stiffened plate girders at Lehigh University has shown that there is no consistent relationship between the ultimate strength of a steel plate girder and the theoretical web buckling strength of the girder.[1,2,3,4] Based on this work specifications for transversely stiffened plate girders for buildings are now being used in this country.[5]

In 1963 a new plate girder research project was started at Lehigh University with the general objective of determining the possible contribution of longitudinal stiffeners to the static load-carrying capacity of plate girders. One phase of this research has been to determine the static bending strength of longitudinally stiffened plate girders. Static bending tests were performed on five longitudinally stiffened plate girders during the summer of 1964. The purpose of this report is to describe the testing of these girders, to report the test results and to present the conclusions of the experimental investigation. The results of a parallel theoretical study will be presented separately in a later report.

2. TEST PROGRAM

2.1 Introduction

The primary objectives of the tests were (1) to determine to what extent longitudinal stiffeners can contribute to the resistance of the web to vertical buckling of the compression flange, (2) to determine how the stress redistribution at loads above the theoretical web buckling load is affected by the presence of a longitudinal stiffener and (3) to determine to what extent lateral web deflections can be reduced by the use of a longitudinal stiffener.

The principal variables describing the geometric and material properties of a longitudinally stiffened plate girder are the aspect ratio α (ratio of panel width to panel depth), web slenderness ratio β (ratio of web depth to web thickness), yield strain ϵ_y (ratio of modulus of elasticity to yield point), longitudinal stiffener position η (distance from compression flange to stiffener divided by web depth), stiffener rigidity ratio γ_s (ratio of stiffener moment of inertia to web moment of inertia) and stiffener area ratio δ_s (ratio of stiffener area to web area). All of these variables are further defined in the Nomenclature. The same type of steel, longitudinal stiffener position and web slenderness ratio were used for all of the specimens, therefore the effects of variation of panel size and longitudinal stiffener size were investigated during the testing program. The actual values of the geometric parameters for the five specimens are listed in Table I.

2.2 Test Specimens

The test setup in general consisted of three major sections, two identical end sections (end fixtures) and the test specimen itself (Fig. 1). The end fixtures and the test specimens were designed so that they could be bolted together thus permitting the same end fixtures to be used with all five test specimens.

The test specimens were 11 ft. 3 in. long. For each specimen the web was 1/8 in. thick and 55 in. deep, the flanges and the end bolting plates were 12 in. wide and 3/4 in. thick, and the transverse stiffeners were 3 in. wide and 1/4 in. thick. Both the longitudinal stiffener and the transverse stiffeners were one-sided. The longitudinal stiffener size and the test panel size (spacing between transverse stiffeners) were varied for each individual test specimen (Fig. 2) such that the longitudinal stiffener size was the only variable for the first three test specimens (LB1, LB2, and LB3) and the panel size was the only variable for test specimens LB2, LB4 and LB5 (Table I).

Several criteria were used in designing the test specimens. The web was selected so as to have a high web slenderness ratio (β range of 400 to 500) while selecting a web plate thickness such that practical size welds could be used. The flanges were designed according to Reference 1, ensuring that neither lateral buckling nor torsional buckling of the compression flange would occur before the yield stress was reached in the flange. The transverse stiffeners were designed

conservatively, exceeding the requirements of both the AISC Specification[5] and the AASHO Specification[6]. Longitudinal stiffener sizes were chosen so as to have a low value of stiffener rigidity ratio ($\gamma_s = 0$, Specimen LB1), an intermediate value ($\gamma_s = 38.4$, Specimens LB2, LB4 and LB5) and a high value ($\gamma_s = 75.1$, Specimen LB3). These various stiffener rigidity ratios are shown in Fig. 3. Also plotted in this figure for comparison purposes are the recommended values of stiffener rigidity ratio according to the German Specifications[7], the British Specifications[8] and the AASHO Specifications[6] (note that the AASHO Specification has been extended above the maximum allowable aspect ratio of 1.0).

The actual dimensions of the component plates of the test specimens (Table II) were obtained from measurements of coupon plates cut from the various plates before fabrication. Figure 4 shows the typical locations of these coupon plates in the specimen component plates. Width and thickness of the flange coupon plates and thickness of the web coupon plates were measured at the points shown in Fig. 5. In all subsequent calculations the average values of thickness and width (Table II) obtained from these measurements were used. Since the material for the longitudinal stiffeners was cut from the web for each specimen, the thickness of the longitudinal stiffener was taken to be the same as that of the web. The nominal values of longitudinal stiffener width and web depth were used in all calculations.

Tensile coupons were cut from each of the coupon plates and tested to determine the material properties of the test specimens. Two tensile coupons were taken from the web coupon plates (one parallel to the direction of rolling and one perpendicular). The static yield strength, percent elongation in 8 in. and the percent reduction in cross-section area obtained from the coupon tests are listed in Table III. Also shown in this table are the chemical properties of the various plates as listed in the mill test reports. The web plates were ASTM A245C material and all other plates were ASTM A36 material.

2.3 Reference Loads

Several reference loads were calculated for each test specimen (Table IV). The first of these, the theoretical web buckling load P_{cr}, is defined by $P_{cr} = \tau_{cr} A_w$, where $\tau_{cr} = k \pi^2 E/12(1-\nu^2)\beta^2$ (Ref. 4). The web buckling coefficient k is dependent on the loading, panel boundary conditions, aspect ratio α and the longitudinal stiffener parameters δ_s and γ_s. Assuming the web panels are simply supported on all sides and using the loading condition of pure bending, the buckling coefficients listed in the second column of Table IV are obtained[9].

The working load P_w was calculated according to the AISC Specification[5], neglecting the presence of the longitudinal stiffener for Specimens LB2, LB3, LB4 and LB5. Nominal values of the cross-section dimensions were used in this calculation, as would be the situation in actual design calculations.

The yield load P_y is defined as the load which causes initiation of yielding in the extreme fiber of the compression flange and is given by $P_y = \sigma_y S_a/120$, where S_a is the moment of inertia of the entire section, including the longitudinal stiffener, divided by the distance from the neutral axis to the extreme fiber of the compression flange. Since P_y is used later to non-dimensionalize the experimentally obtained ultimate load of each girder, measured values of the yield point and cross-section dimensions were used in the calculation.

2.4 Test Setup

As previously explained, the test setup consisted of two identical end fixtures bolted to a test specimen. The end fixtures were designed to resist the combined effects of the shear forces and bending moments present (refer to references 2 and 3 for design criteria). Figure 6 shows the actual size of the end fixtures used whose function was to transfer the bending stresses from the loading system to the test specimen.

The bolted joint (Fig. 6) was designed to transmit the bending stresses from the end fixtures to the test specimen. High strength steel bolts (1 in. diameter) were torqued to a stress of approximately 10,000 ksi except for the bottom eight bolts in each joint which were torqued to approximately 50,000 ksi (approximate yield stress of the bolts). This system of torquing the bolts permitted the reuse of the top ten bolts of each joint.

All of the test specimens, with the exception of Specimen LB5, had three separate panels (Specimen LB5 had four panels). Specimens LB1 through LB4 had one test panel (center panel) and two adjacent side panels (Fig. 2) while Specimen LB5 had two test panels and two side panels (Fig. 2). The function of these side panels was to further distribute the bending stresses throughout the depth of the girder.

The only measurements taken outside of this test panel (center panel) were level readings at the supports which were used to correct the center line deflection readings for support settlement. All other test data was obtained from the test panel only. Therefore any portion of the test setup outside of the center test panel was considered to be part of the loading system and any failure in these sections was not considered as a failure of the test specimen.

The loading system consisted of two 220 kip Amsler hydraulic jacks. These jacks were supplied with oil fed through a common distributor by an Amsler Pendulum Dynamometer which measured the load (P) which was present on one hydraulic jack only. The loading system and the test setup are shown in Fig. 7.

Intermittent lateral support of the compression flange was provided by 2 ½ in. diameter pipes which were pinned to the test specimen and the loading fixtures at one end and to a lateral support beam at the other end. This pinned arrangement allowed the test specimen to move in a vertical direction only, restraining lateral movement in either direction. The lateral supports were located at the transverse stiffeners which bounded the test panel (center panel), at the bolted joints and at the loading points.

During the testing of the five specimens certain modifications of the loading fixtures were required to obtain a satisfactory transfer of stress to the center test panel. Reinforcing plates were required at the bottom of the bolted joint (Fig. 8) to prevent excessive deformation of the end plates of the test specimen. This excessive deformation caused additional bending stresses in the bottom bolts and led to failure of the bottom two bolts in the first test of the series. Reinforcement was also required at the compression flange in the side panels (Fig. 8) to prevent yielding of the compression flange in this zone (side panels) before it was obtained in the test panel compression flange. After

this additional reinforcement was added no further difficulties were experienced and all failures occurred in the center panel of the test specimen.

3. TEST PROCEDURE AND RESULTS

3.1 Introduction

The objective of this chapter is to describe in detail the testing procedure, general girder behavior and the test results for each of the five specimens. The test results consist primarily of load-deflection diagrams, web deflection diagrams, strain distribution plots and the observed ultimate loads. A specimen was considered to have reached its ultimate load when a substantial increase in the center line deflection was observed with no accompanying increase in the applied loads.

In the following discussion a coordinate system will be used to identify points of importance on the test girders. The origin is at the geometric center of the web of each specimen, with the x-axis in the longitudinal direction, the y-axis in the transverse direction and the z-axis in a direction perpendicular to the plane of the web (see Nomenclature). The side of the specimen in the positive z direction will be called the near side of the specimen and the negative z direction side will be referred to as the far side. Thus all the longitudinal stiffeners were on the near side and all the transverse stiffeners were on the far side.

3.2 General Girder Behavior

The testing history and general behavior of any one test specimen can be traced with the aid of the load-versus-center line deflection curve for the particular specimen (Figs. 9 through 13). The applied load P on each hydraulic jack was measured as explained previously and the vertical deflection at the center line of the specimen (v_{ℓ}) was measured with a dial gage mounted on the floor of the test bed. The dial gage readings provided a control on the testing speed, gave an indication of the behavior of the specimen during testing and were also used to determine when the ultimate load had been attained. Scales mounted on the bearing stiffeners at the supports were read with an engineer's level to determine the support settlements. These support settlement readings have been used to correct the center line deflection readings which are plotted in Figs. 9 through 13.

In the P-v_{ℓ} curves (see for example Fig. 11) the load P is plotted as the ordinate and the corrected center line deflection is plotted as the absissa. Also shown in the figure is a schematic drawing of the straight and deformed test girder with the two applied loads (P). The numbered circles indicate positions on the curve where the loading was stopped and where measurements were taken. These positions are referred to by the load numbers next to the circles. The values of the reference loads (P_w and P_{cr}) are also plotted along with the observed ultimate load (P_{ult}).

The first loading cycle consisted of loading the test specimen until inelastic behavior was observed (indicated by a substantial increase in deflection per unit load) and then returning to zero load. A second cycle was then started and continued until the ultimate load of the test specimen was attained. In any welded structure residual stresses are present which affect measurements to the extent that readings taken during an initial loading cycle may be misleading.[10] The first loading cycle was intended to partially relieve the effects of the residual stresses on the measurements taken during the second cycle.

Initially (Fig. 11, load Nos. 1 through 14), web deflections and strain measurements were taken at load increments which were selected to insure that at least seven such sets of readings were obtained. In the inelastic range (Fig. 11, load Nos. 15 through 20) the procedure was to load the specimen until a certain predetermined center line deflection was obtained and then to allow the load to stabilize as the deflection was held constant. All measurements were taken after the load had stabilized. This same procedure was followed in all the test specimens except Specimen LB2, where the load was held constant in the inealstic range and the center line deflection was allowed to increase until it stabilized (Fig. 10, load Nos. 15 through 18). This procedure required an excessive waiting period until the center line deflection had stabilized and therefore it was not used in testing the other specimens.

3.3 Strain Distribution

Strain measurements were taken at the center line of the test panel (x = 0) for the various load points, using electrical resistance strain gages mounted at the positions shown in Fig. 14. The measured strains at four different loads are plotted to show the strain distribution throughout the depth of each test specimen (Figs. 15 through 19). Using Specimen LB3 as an example (Fig. 17) a typical strain distribution plot will be explained.

The various strain gage positions are shown in Fig. 17 and at each of these positions is plotted the average strain at the center of the web, obtained by averaging the data from the two gages on the web surface, for loads of 0^k (second load cycle), 80^k, 120^k and the ultimate load. The plotted points have been connected by straight lines. In a separate graph (same figure) the variation in strain at two points (labeled A and B) can be traced from a load of 0^k (second cycle) to the ultimate load. In this plot the strain is plotted as the absissa and the load P as the ordinate.

3.4 Web Deflection

Lateral web deflections were measured at several cross sections in the test panel (center panel) for the various load points, using a specially designed device. This device consisted of a portable rigid truss to which dial gages were attached at certain y-coordinate points

(Fig. 20). By placing the measuring device at various x-coordinate stations and reading the gages (y-coordinates) the deflected configuration of the entire test panel web was obtained. Reference measurements were taken after every set of readings (using a milled steel surface) to check against accidental movement of the various dial gages. The deflected web shapes are given for the five test specimens in Figs. 21 through 25 and Specimen LB3 (Fig. 23) will again be used to explain a typical web deflection plot.

The measured deflections were plotted at the various y-coordinate points and then connected with straight lines. The deflected shapes shown in Fig. 23 are for load Nos. 8, 12, 14 and 20 (0^k, 80^k, 120^k and ultimate load). The inserted sketch of the test panel locates the cross sections A and B where the web deflections were taken. The two graphs on the right show the rate at which the lateral deflections increased at the longitudinal stiffener during the second load cycle (load Nos. 8 through 20). The measured deflection is plotted as the absissa and the load P as the ordinate.

3.5 Ultimate Loads and Modes of Failure

Specimen LB1

Two separate tests were conducted on this specimen. In the first test, which was also the first test in the program, a failure occurred outside the test panel (center panel), at the bolted joint. The second test, which was the fifth test in the series, consisted of

testing the same specimen after it had been reinforced as previously explained. In this test, yielding of the compression flange was first observed between load Nos. 36 and 37 and the ultimate load attained was 156.5 kips. General yielding of the compression flange (yielding throughout the entire flange thickness) was the factor which determined the ultimate load. There were also indications of possible torsional buckling of the compression flange.

Figure 26 shows the completely yielded compression flange in the test panel area after the second test, as viewed from below the compression flange on the near side. Figure 27 shows the tendency toward torsional buckling of the compression flange and it also clearly shows that yielding had penetrated throughout the thickness of the flange. The yield line patterns across the width of the compression flange can be seen in Fig. 28. The effectiveness of the reinforcement outside of the test panel is demonstrated in this figure by the absence of yield lines in the reinforced area.

Specimen LB2

This specimen was reinforced in the bolted joint area before testing to prevent a bolt failure similar to that which occurred in the first test on Specimen LB1. Yielding of the compression flange was first observed at load No. 15 and yielding of the longitudinal stiffener began to occur at load No. 17. The ultimate load of this specimen was 152.0^{k} with the controlling factor again being general yielding of

the compression flange. This yielding occurred outside of the test panel (in the side panels) however, and when the specimen was strained beyond the ultimate load vertical buckling of the compression flange occurred in the yielded portion. A second test was attempted after reinforcing the compression flange in the side panel areas but the reinforced specimen was unable to sustain loads as high as those in the first test.

Figure 29 shows the vertical buckle as viewed from the near side of the specimen. Buckles in the longitudinal stiffener are also evident in this photo. Figures 30 and 31 show the extent of yielding in the compression flange and also the damage to the web of the specimen. Figure 30 was taken from the near side of the specimen while Fig. 31 was taken from the far side.

Specimen LB3

As a result of the behavior of the first two specimens. Specimen LB3 was reinforced at both the compression flange (in the side panel zones) and the bolted joint before it was tested. The compression flange was first observed to yield at load No. 15. Yielding and buckling of the longitudinal stiffener occurred at load No. 19. The ultimate load for the specimen was 150^{k} with general yielding of the compression flange being the controlling factor.

In Fig. 32 the extent of yielding in the compression flange after the test is clearly shown. Buckling of the longitudinal stiffener is also evident in this figure (view is from the near side of the specimen). Figures 33 and 34 show the yield patterns present across the width of the compression flange and also the buckled shape of the longitudinal stiffener (Fig. 33).

Specimen LB4

Specimen LB4 was reinforced before testing in the same manner as was Specimen LB3. First yielding of the compression flange occurred at load No. 15, deformation of the longitudinal stiffener began to occur between load Nos. 15 and 16 with the longitudinal stiffener buckling at load No. 18. The ultimate load attained for this specimen was 147^{k} with general yielding of the compression flange being the controlling factor. A tendency toward lateral buckling of the compression flange was also evident in the test panel zone. The specimen was then strained beyond the ultimate load and vertical buckling of the compression flange occurred in the test panel.

Figures35 and 36 show the yielded compression flange after ultimate load was reached. Also visible in Fig. 35 are the buckles in the longitudinal stiffener. In Fig. 36 the tendency toward lateral buckling can be seen from the distribution of yield lines in the compression flange. Figures 37 and 38 show the specimen after vertical buckling occurred. Extensive damage to the web is clearly shown in each figure. Figure 37 is viewed from the near side and Fig. 38 from the far side.

Specimen LB5

Specimen LB5 was reinforced in the same manner as Specimens LB3 and LB4. First yielding of the compression flange occurred at load No. 15 and bending of the longitudinal stiffener began between load Nos. 17 and 18. At load No. 21 the longitudinal stiffener was severely buckled. The ultimate load of the specimen was 150.8^{k} with general yielding of the compression flange in the two test panels again controlling.

Figure 39 shows the yielded compression flange and the severely buckled longitudinal stiffener as seen from the near side of the specimen. Figure 40 shows the compression flange as viewed from the far side. The two test panels are also clearly shown by this photo. Figure 41 shows the yield line patterns present across the width of the compression flange in both test panels.

4. DISCUSSION

One of the strongest impressions left by the tests was the similarity in the behavior of the specimens which had longitudinal stiffeners (Specimens LB2, LB3, LB4 and LB5). For each of the girder specimens a definite sequence of events leading to the attainment of ultimate load can be traced. Local yielding of the compression flange was the first observed event in this sequence. As the applied loads were increased, yielding and then local buckling of the longitudinal stiffener occurred. Finally, the compression flange became completely yielded and at this stage the ultimate load was reached.

Previous research has demonstrated that the bending strength of a transversely stiffened plate girder is not directly related to the theoretical web buckling load[1,2,3,4]. The tests described in this report have shown that there is no rational correlation between the theoretical web buckling load and the bending strength of a longitudinally stiffened plate girder. Buckling theory predicts that the critical load for the specimens with longitudinal stiffeners is over five times that of the specimen without a longitudinal stiffener (Table V). However, the ultimate loads of all of the test specimens are of about the same magnitude and actually, the highest ultimate load was reached in the test of the specimen with no longitudinal stiffener.

One of the main objectives of the tests was to determine to what extent longitudinal stiffeners can contribute to the resistance of the web to vertical buckling of the compression flange. Vertical buckling of the compression flange did occur in two of the specimens (LB2 and LB4), but only after the ultimate load had been attained and the compression flange had been subjected to additional straining. Since the ultimate load for all of the test specimens was reached as a result of general yielding of the compression flange, it appears that the phenomenon of vertical buckling can only be expected to occur after the ultimate load has been reached. Therefore, the effect of the longitudinal stiffeners on vertical buckling can only be measured by how much the stiffeners affected the ultimate loads. In the last column of Table V, the experimentally obtained ultimate loads have been divided by the corresponding yield loads to eliminate small differences in the dimensions and material properties among the specimens. A comparison of this P_{ult}/P_y ratio for the five test girders indicates that the longitudinal stiffeners had little, if any, influence on the magnitude of the ultimate loads.

It has been observed in tests on transversely stiffened plate girders[1,4] that, at loads above the theoretical web buckling load, a redistribution of stress from the compressed portion of the web to the compression flange takes place. As is evident from the strain distribution plots in Fig. 15, this stress redistribution also occurred in

Specimen LB1. The effect of the longitudinal stiffeners of Specimens LB2 to LB5 on the strain distribution can be seen in Figs. 16 through 19. At loads up to P_w and above, the measured strain distributions were quite close to the linear distribution predicted by beam theory. Only after a longitudinal stiffener had buckled did a significant redistribution of strain to the compression flange occur, and even at this point, the strain at the stiffener was markedly higher than it would have been at the same position if no stiffener were present. In most cases the strain at the stiffener reached or exceeded the yield strain by the time that the ultimate load had been reached.

Another objective of the test program was to determine to what extent lateral web deflections can be reduced by the use of a longitudinal stiffener. The effectiveness of the longitudinal stiffeners of Specimens LB2 through LB5 can be judged qualitatively with the aid of Figs. 22 through 25, but a more accurate evaluation of the stiffener's ability to control web deflections can be made with the information presented in Table VI. In the fourth column of the table, listed for each girder, is the maximum value of lateral web deflection which was measured at the longitudinal stiffener at the working load, $(w_w)_{max}$. In the next column is listed the deflection measured at the same position when the applied load was zero, w_o. The percent increase in lateral web deflection between zero load and the working load is given by $\Delta_w = \left[(w_{w_{max}} - w_o)/w_o\right] \times 100$ and is listed in the last column of Table VI. Since Δ w for Specimen LB1 with no longitudinal stiffener is 140% while

the largest value of Δw for the four girders with longitudinal stiffeners is only 40%, it is evident that the stiffeners were very effective in controlling web deflections at the working load. As can be seen from Figs. 22 through 25, the web deflections increase rapidly only after a stiffener had buckled.

The effect of the principal test variables, aspect ratio (α) and stiffener rigidity ratio (γ_s), can also be evaluated from Table VI. From the data for the three specimens with a constant aspect ratio of 1.0 and with varying stiffener rigidities (Specimens LB1, LB2 and LB3) it is seen that larger stiffener rigidities result in more effective web deflection control. Aspect ratio influences the effectiveness of a stiffener in that it determines the distance the stiffener must span between transverse stiffeners. Thus, for Specimens LB2, LB4 and LB5, which had the same stiffener rigidity but different aspect ratios, the specimen with the largest aspect ratio was least effective in controlling web deflections.

In summary, the tests demonstrated that longitudinal stiffeners can be very effective in controlling lateral web deflections and in maintaining a linear strain distribution up to the point where local buckling of the stiffener occurs. However, for the stiffener sizes used in these tests, no significant effect on the magnitude of the ultimate load was apparent. A discussion of the proportioning of longitudinal stiffeners and of predicting the bending strength of longitudinally stiffened plate girders will be presented separately in a later report.

5. CONCLUSIONS

From the experimental work on five longitudinally stiffened plate girders described in this report, the following conclusions can be formulated:

1. There is no rational correlation between the theoretical web buckling load and the bending strength of a longitudinally stiffened plate girder.
2. In all of the tests, the ultimate load was reached as a result of general yielding of the compression flange.
3. Vertical buckling of the compression flange was observed in two tests; in both cases this occurred when the specimen was strained beyond the ultimate load.
4. The longitudinal stiffeners which were used in these tests had no significant effect upon the observed ultimate loads of the girders.
5. The longitudinal stiffeners had a significant effect upon the strain redistribution in the girders, causing the strain distribution to remain approximately linear until the longitudinal stiffener buckled.
6. The longitudinal stiffeners were very effective in controlling web deflections up to the loads at which the stiffeners buckled.

6. NOMENCLATURE

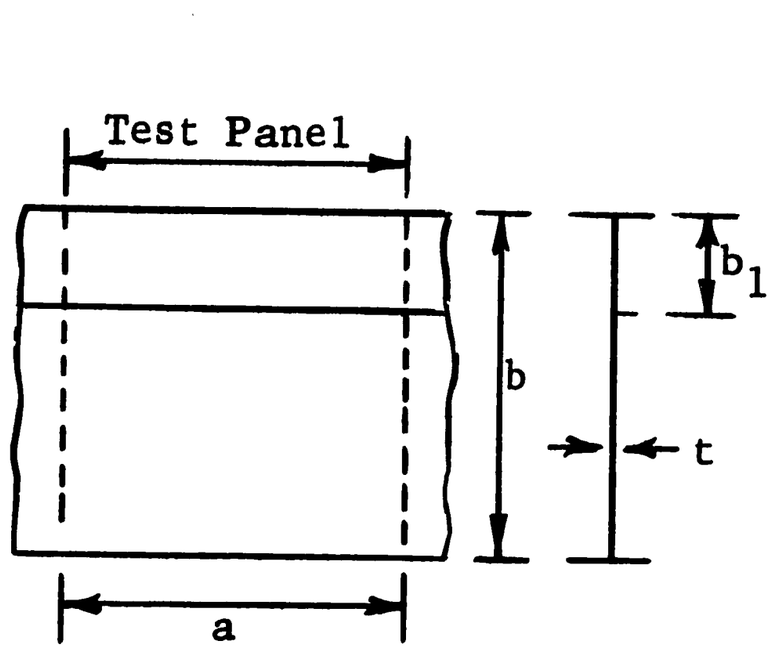

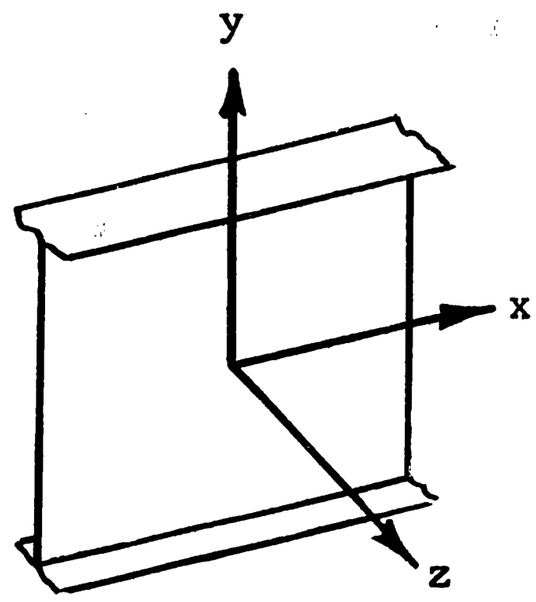

a	panel length
b	web depth
b_1	distance from top flange to center of longitudinal stiffener
k	web buckling coefficient
t	web thickness
v	deflection in the negative y - direction
w	deflection in the positive z - direction
x,y,z	cartesian coordinate axes
A_s	longitudinal stiffener area
A	web area
E	modulus of elasticity (29.6 ksi)
I_s	longitudinal stiffener moment of inertia
P	load applied by one hydraulic jack
P_{cr}	theoretical web buckling load

P_{ult} experimentally obtained ultimate load

P_w working load

P_y load which causes yielding in extreme fiber of compression flange.

S_a moment of inertia of entire section, including longitudinal stiffener, divided by distance from neutral axis to extreme fiber of compression flange

α aspect ratio, a/b

β slenderness ratio, b/t

γ_s stiffener rigidity ratio, $12\ (1-\nu^2)\ I_s/bt^2$

δ_s stiffener area ratio, A_s/bt

ϵ strain, σ/E

ϵ_y yield strain σ_y/E

η longitudinal stiffener position b_1/b

ν Poisson's Ratio (0.3)

σ stress, ϵE

σ_y yield stress, $\epsilon_y E$

7. TABLES AND FIGURES

Table I Test Specimen Parameters

Specimen	α	β	γ_s	η	δ_s
LB1	1.0	444	0	0.2	0
LB2	1.0	447	38.4	0.2	0.0364
LB3	1.0	447	75.1	0.2	0.0455
LB4	1.5	447	38.4	0.2	0.0364
LB5	0.75	447	38.4	0.2	0.0364

Table II Plate Dimensions

Specimen	Comp. Flg.		Tension Flg.		Web		Long. Stiffener	
	Thick-ness	Width	Thick-ness	Width	Thick-ness	Depth*	Thick-ness	Width*
LB1	0.754	12.00	0.756	12.00	0.124	55.0	--	--
LB2	0.753	11.99	0.755	12.03	0.123	55.0	0.123	2.0
LB3	0.752	12.00	0.752	12.00	0.123	55.0	0.123	2.5
LB4	0.753	11.98	0.754	12.00	0.123	55.0	0.123	2.0
LB5	0.758	12.00	0.757	12.02	0.123	55.0	0.123	2.0

* Not measured on coupons directly - taken as nominal values

Table III Material Properties

Specimen	Component	σ_y ksi	% Elongation (in 8 in.)	% Area Reduction	Chemical Composition			
					C	Mn	P	S
LB1	Comp. flg.	37.6	29.0	54.3	.25	.67	.018	.023
	Web*	33.3	28.2	47.8	.16	.62	.010	.025
	Tens. flg.	37.4	29.6	51.6	.25	.67	.018	.023
LB2	Comp. flg.	37.0	27.6	54.0	.25	.67	.018	.023
	Web*	34.1	28.7	43.3	.16	.62	.010	.025
	Tens. flg.	37.1	28.2	57.1	.25	.67	.018	.023
LB3	Comp. flg.	36.0	30.0	55.2	.25	.67	.018	.023
	Web*	34.5	27.4	42.5	.16	.62	.010	.025
	Tens. flg.	36.1	25.6	50.2	.25	.67	.018	.023
LB4	Comp. flg.	34.9	30.8	53.5	.25	.67	.018	.023
	Web*	35.8	29.6	45.0	.16	.62	.010	.025
	Tens. flg.	35.9	29.8	53.5	.25	.67	.018	.023
LB5	Comp. flg.	35.3	27.0	50.7	.25	.67	.018	.023
	Web*	35.6	30.2	48.4	.16	.62	.010	.025
	Tens. flg.	35.5	29.9	51.8	.25	.67	.018	.023

* Web values are average values of the two tensile coupons

Table IV Reference Loads

Specimen	k	P_{cr} (kips)	P_w (kips)	P_y (kips)
LB1	23.9	15.1	91.8	175.7
LB2	129.4	81.3	91.5	172.2
LB3	129.4	81.4	91.5	169.1
LB4	129.4	81.1	91.5	163.8
LB5	129.4	81.7	91.6	166.5

Table V Test Results

Specimen	Variables		Reference Loads			Test Results	
	α	γ_s	P_{cr}	P_w	P_y	P_{ult}	P_{ult}/P_y
LB1	1.0	0	15.1	91.8	175.7	156.5	.890
LB2	1.0	38.4	81.3	91.5	172.2	152.0	.883
LB3	1.0	75.1	81.4	91.5	169.1	150.0	.887
LB4	1.5	38.4	81.1	91.5	163.8	147.0	.897
LB5	0.75	38.4	81.7	91.6	166.5	150.8	.905

Table VI Web Deflection Comparison

Specimen	α	γ_s	$(w_w)_{max}$ (in.)	w_o (in.)	Δw %
LB1	1.0	0	0.221	0.092	140
LB2	1.0	38.4	0.215	0.186	16
LB3	1.0	75.1	0.256	0.225	14
LB4	1.5	38.4	0.232	0.166	40
LB5	0.75	38.4	0.076	0.065	17

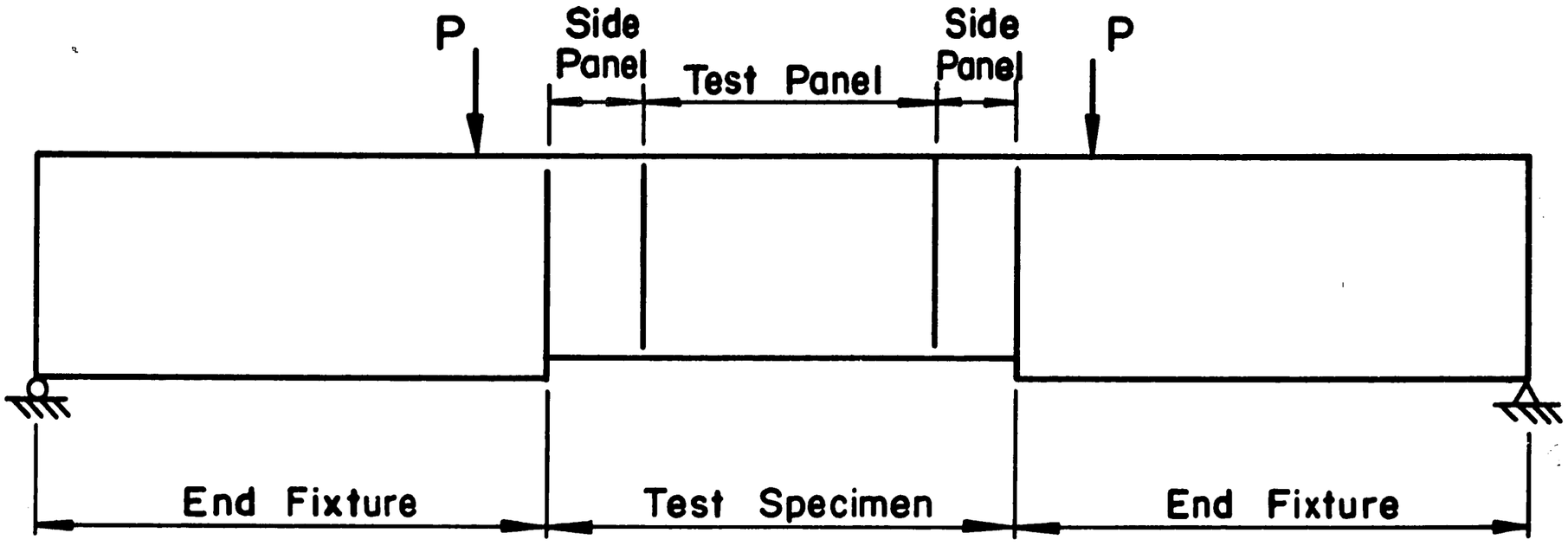

Fig. 1 Schematic Test Setup

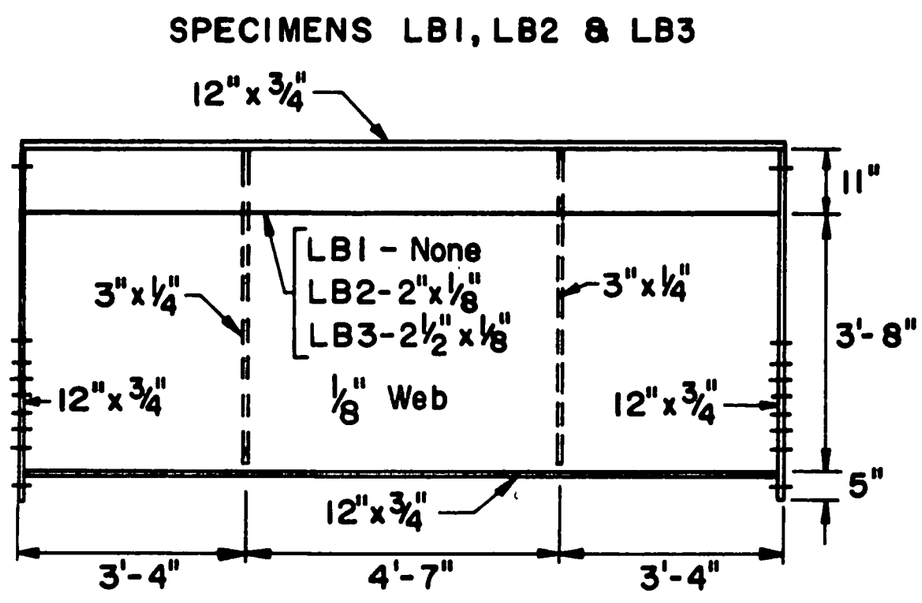

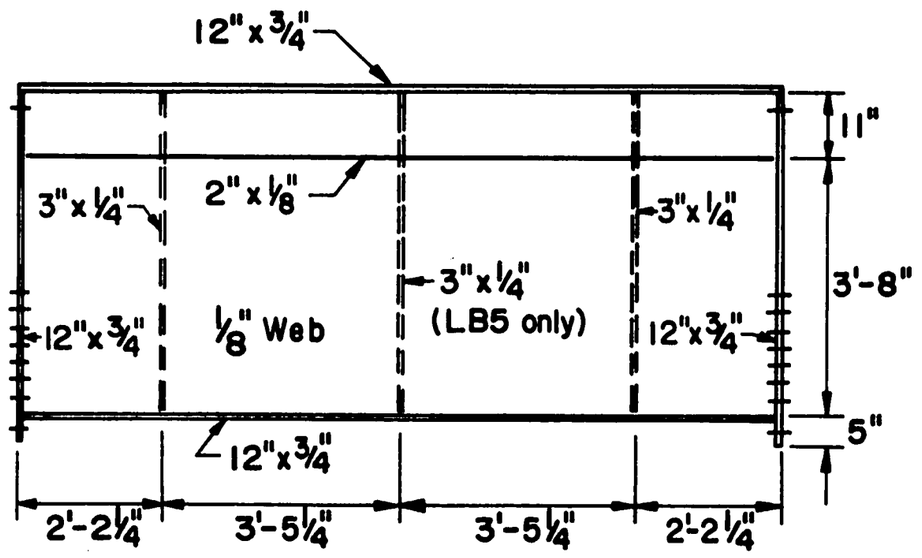

Fig. 2 Test Specimens

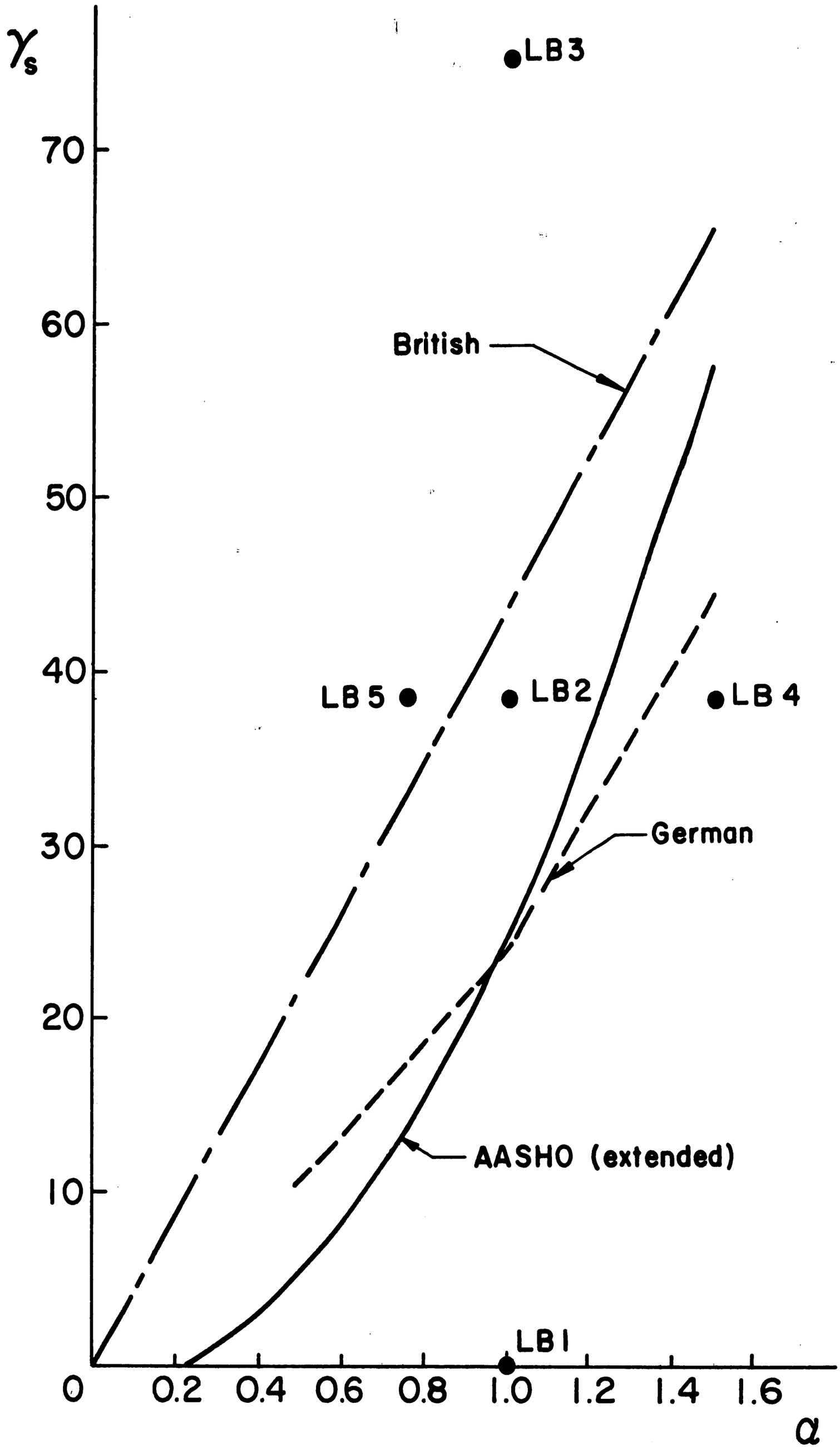

Fig. 3 Test Specimen Parameters

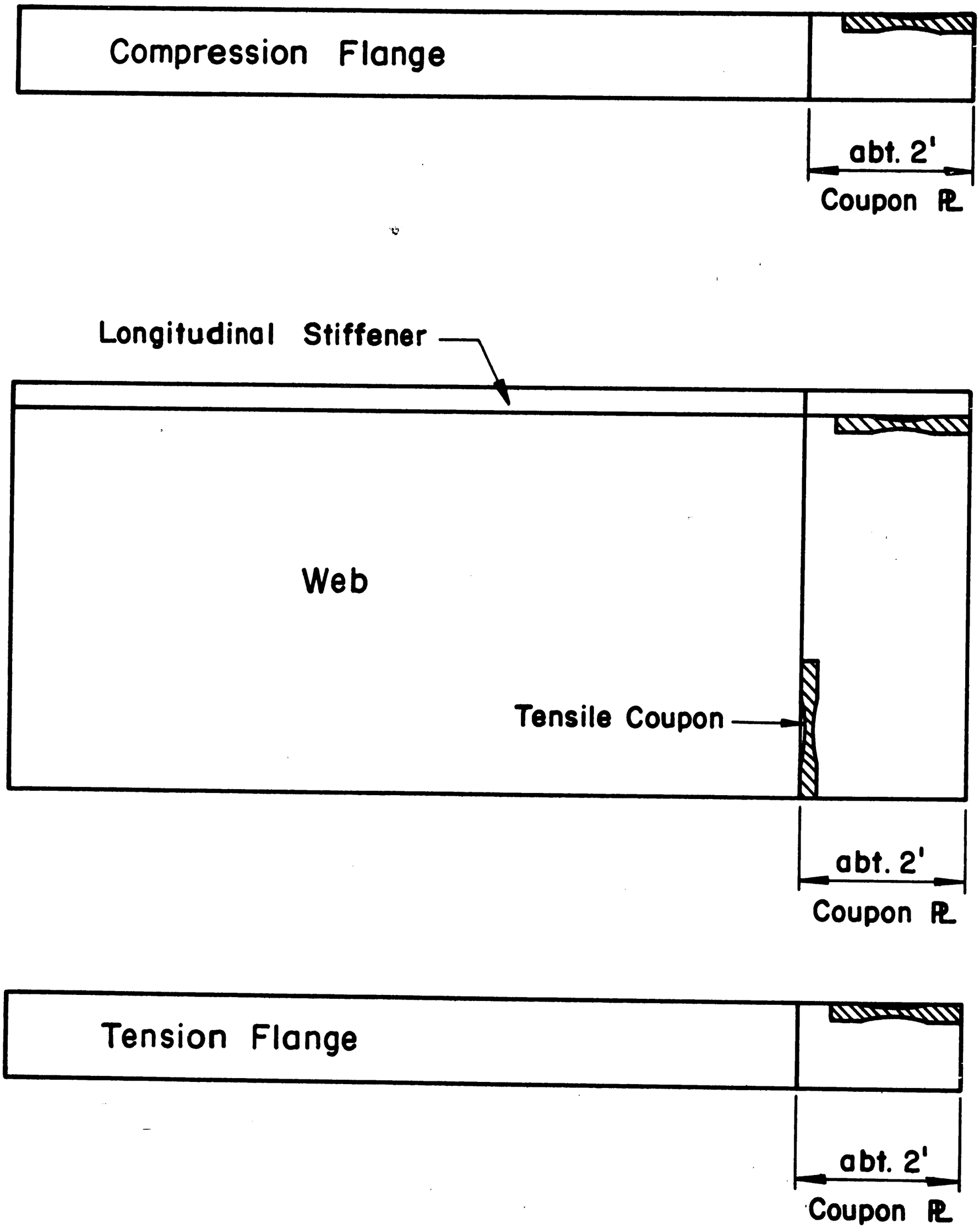

Fig. 4 Typical Locations of Coupon Plates

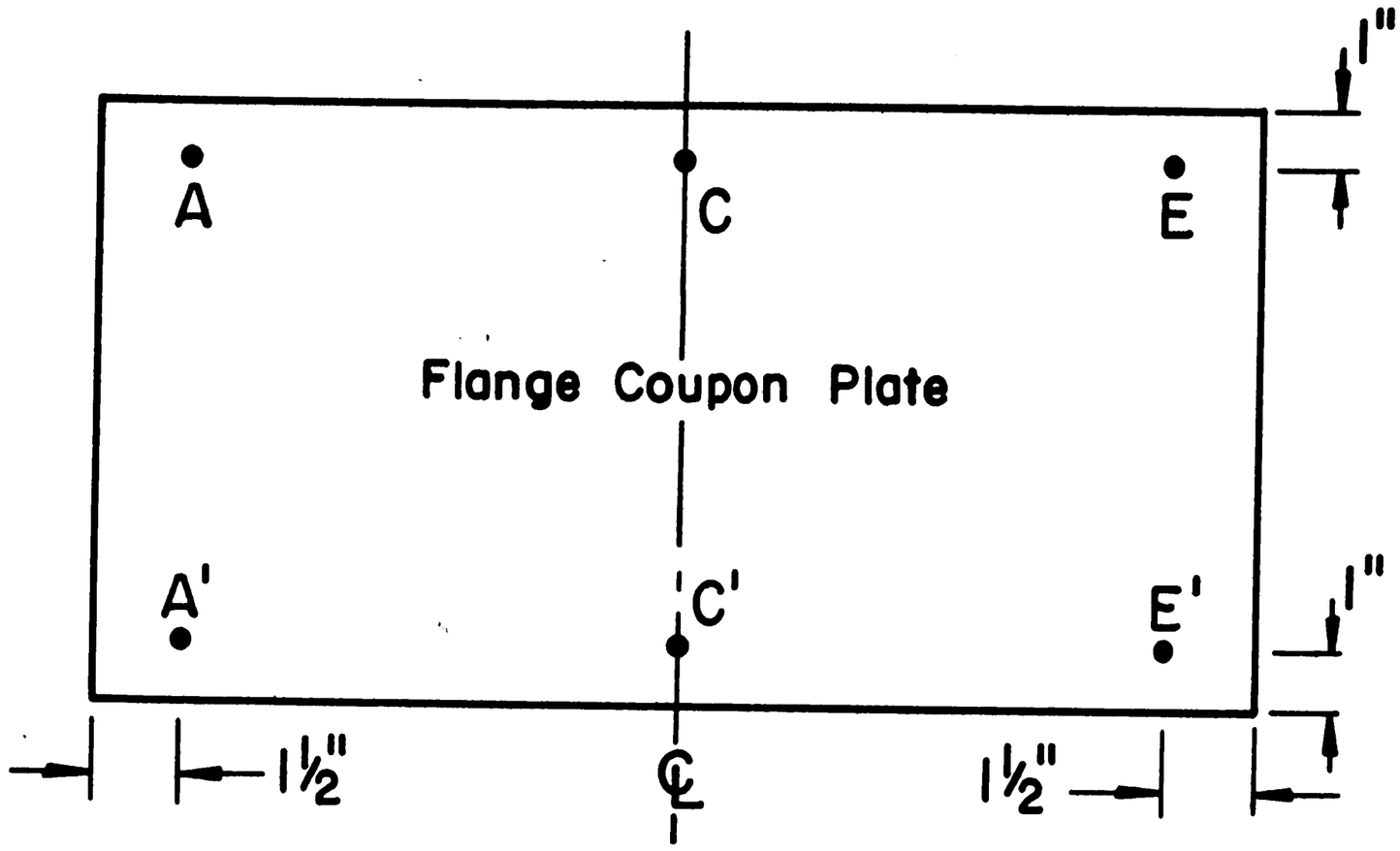

Thickness at A, A', C, C', E, E'
Width at A-A', C-C', E-E'

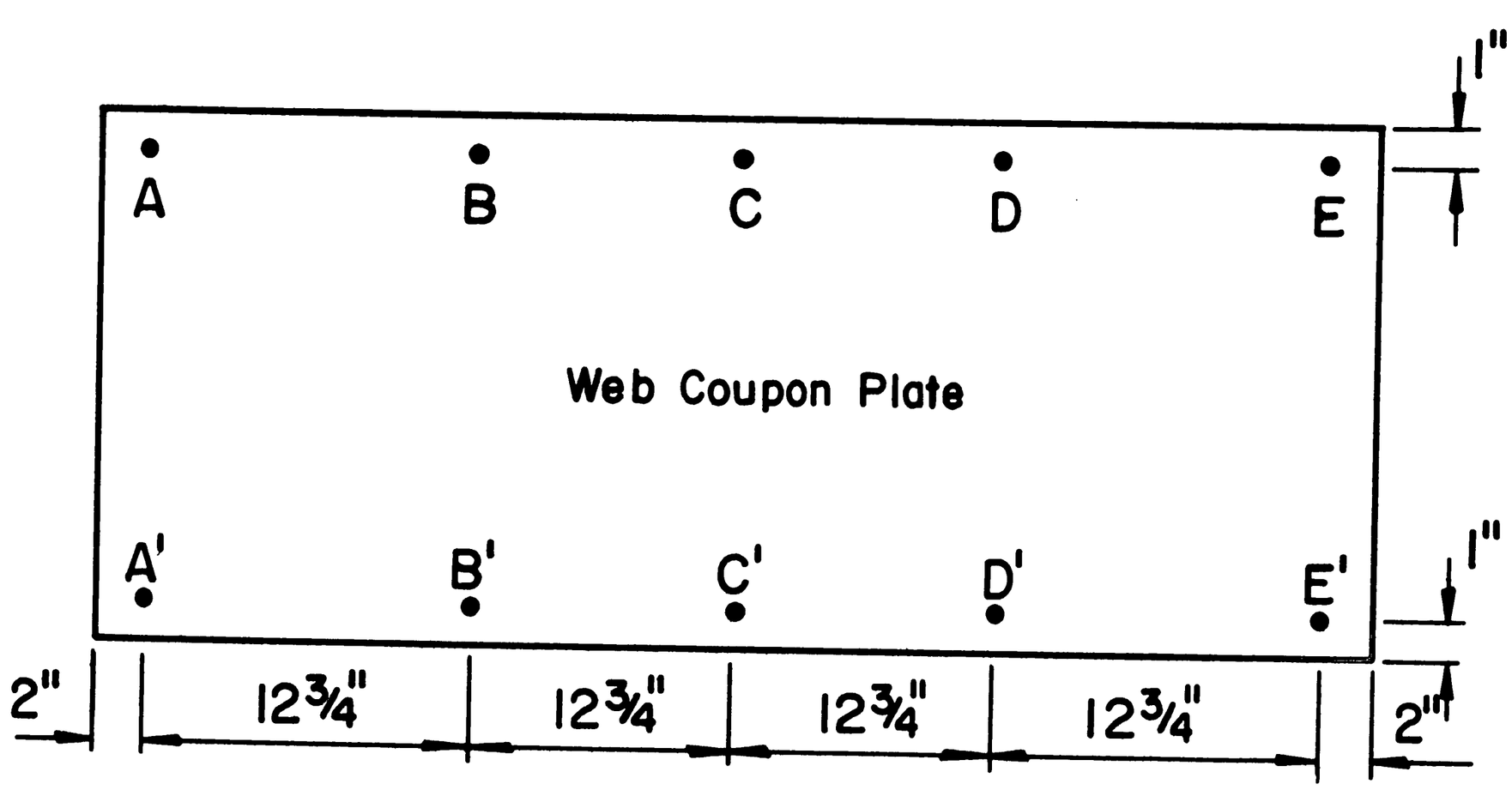

Thickness at A, A', B, B', C, C', D, D', E, E'

Fig. 5 Location of Coupon Plate Measurements

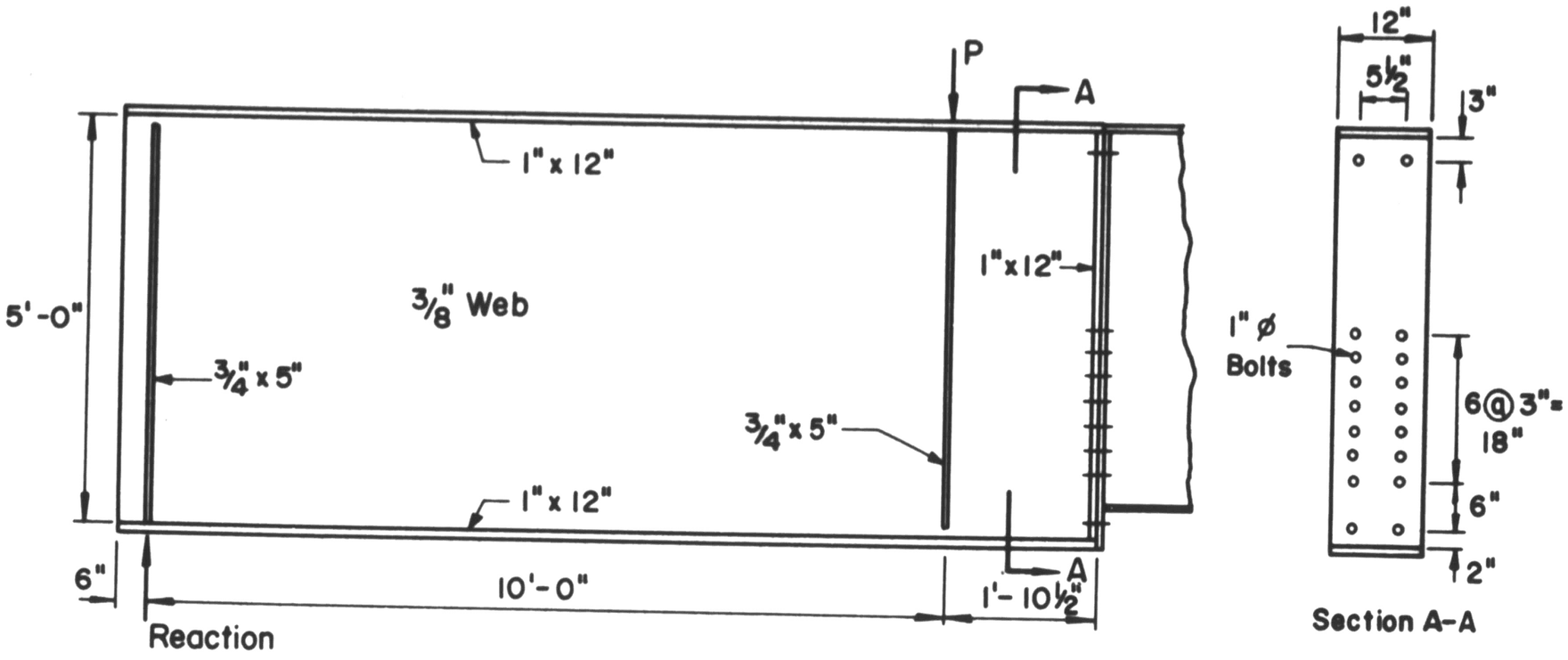

Fig. 6 End Fixture and Bolted Joint

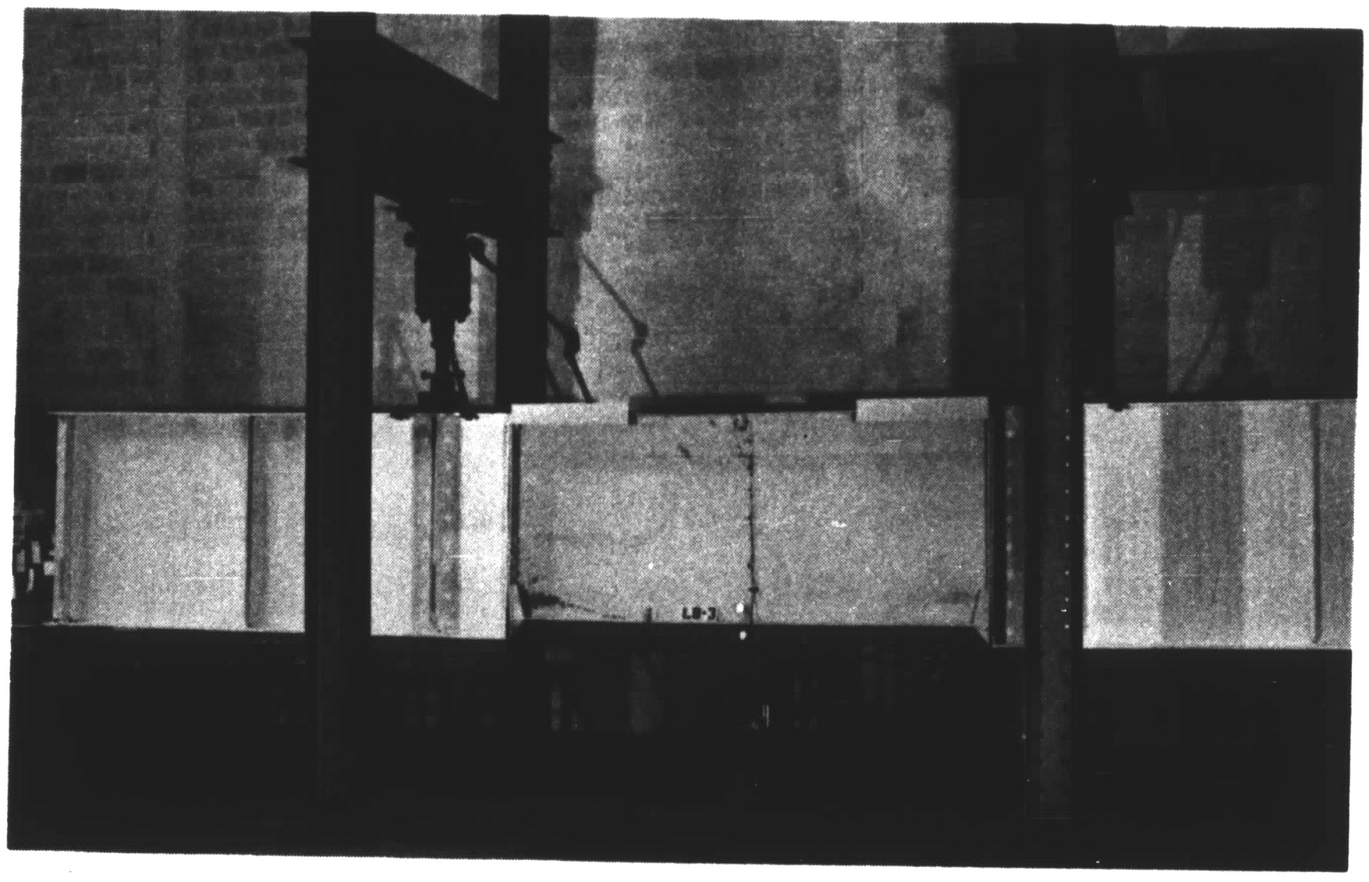

Fig. 7 Test Setup

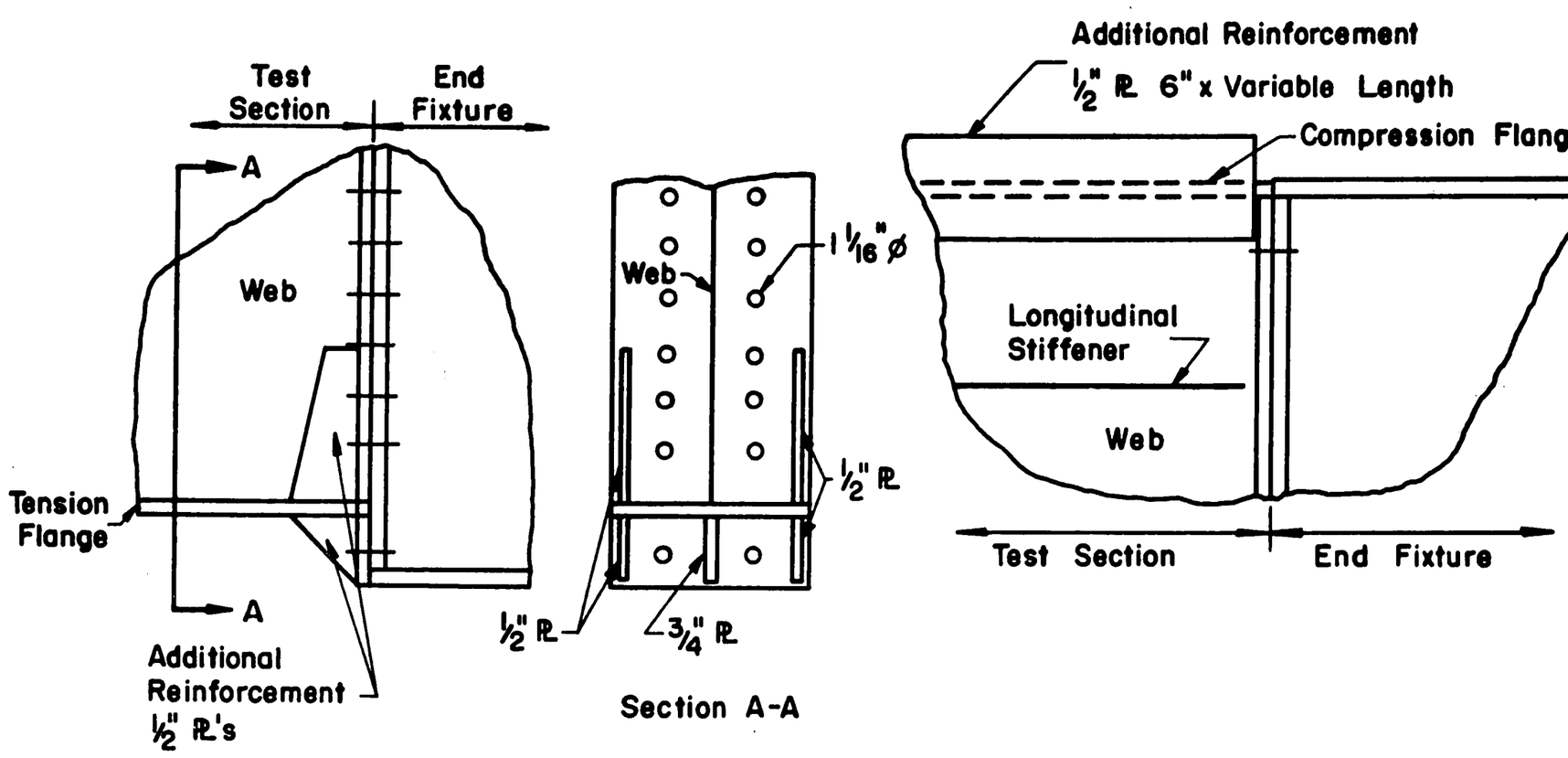

Fig. 8 Reinforcement of Side Panels

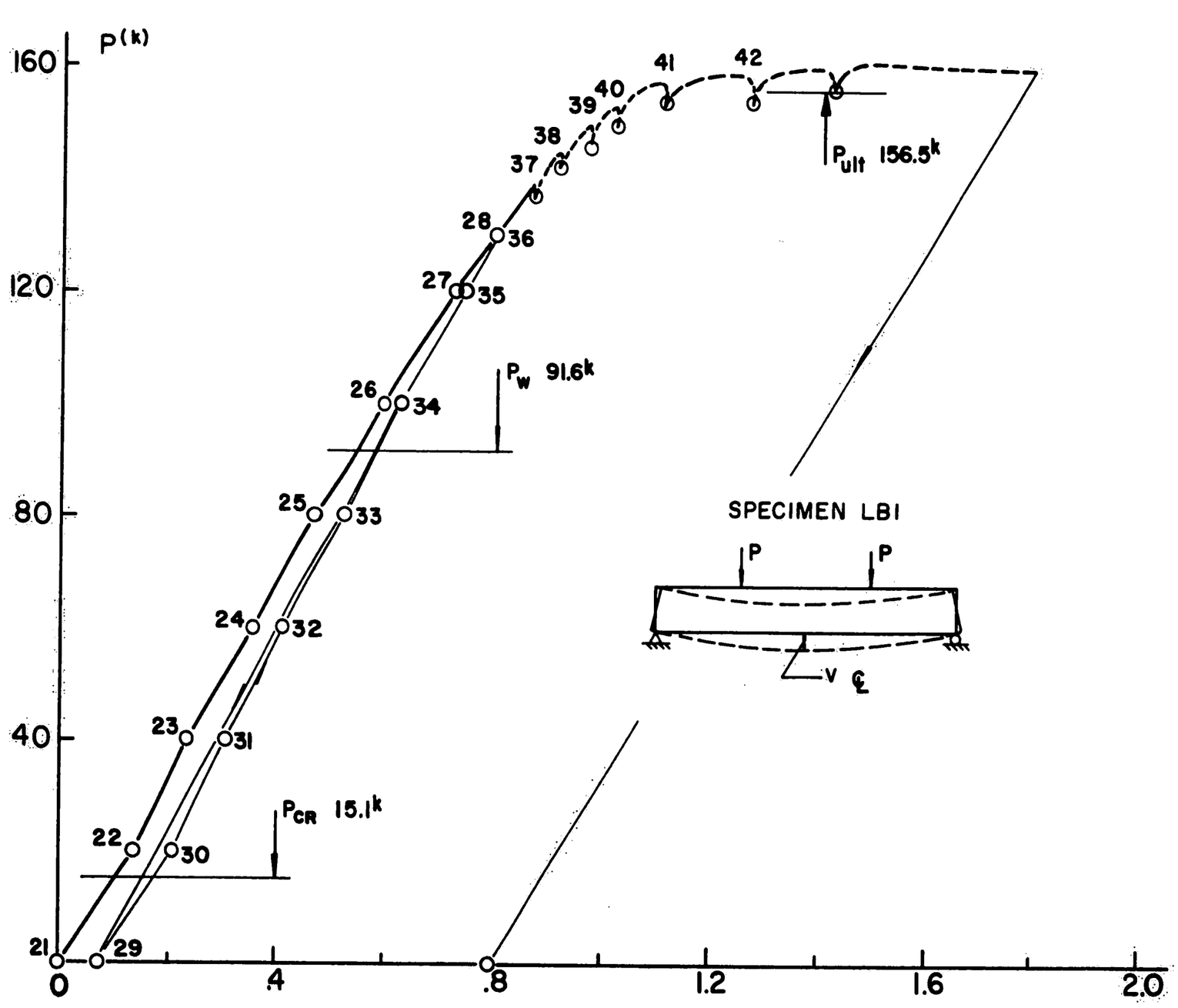

Fig. 9 Load-Vs-Centerline Deflection Curve

(Specimen LB1)

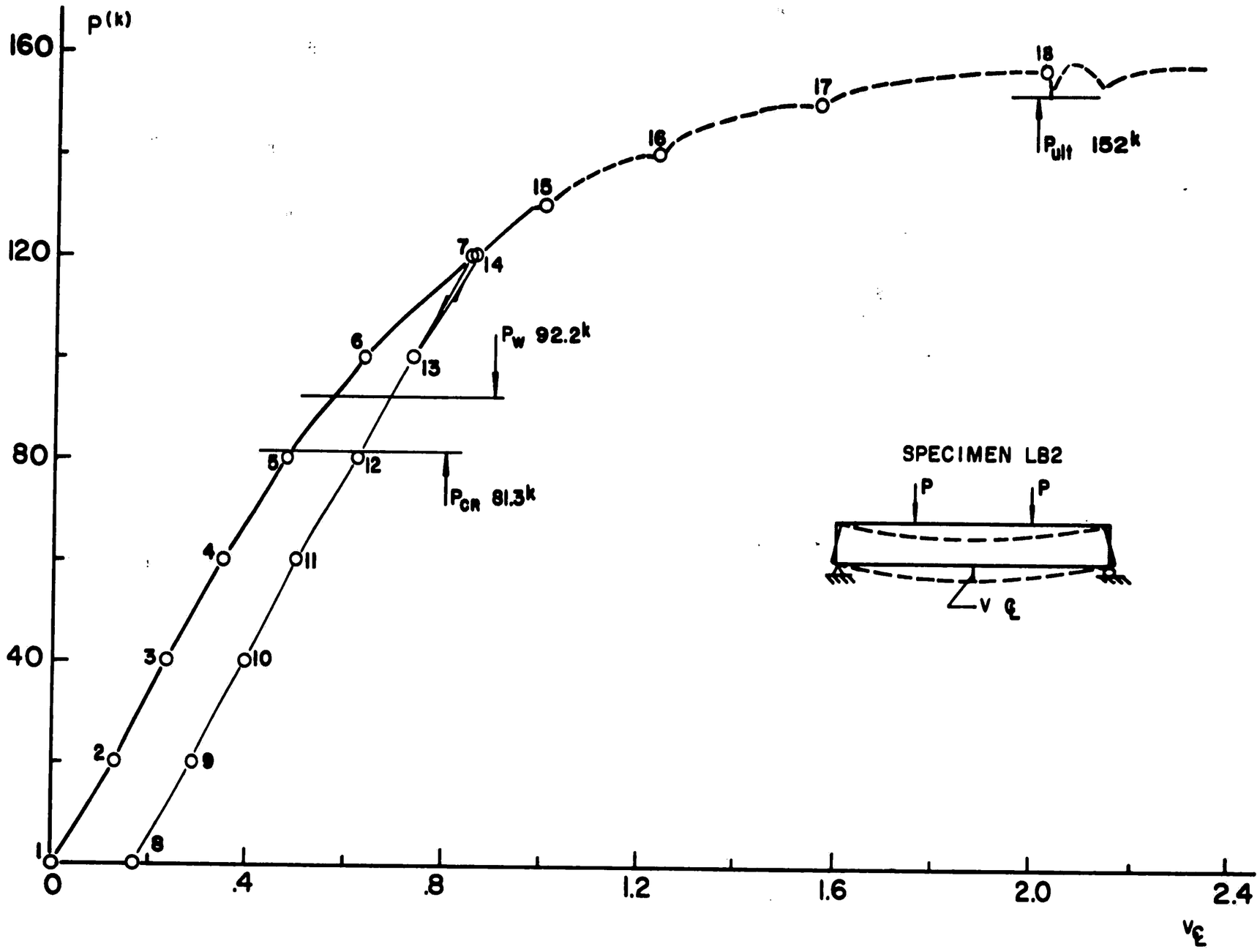

Fig. 10 Load-Vs-Centerline Deflection Curve

(Specimen LB2)

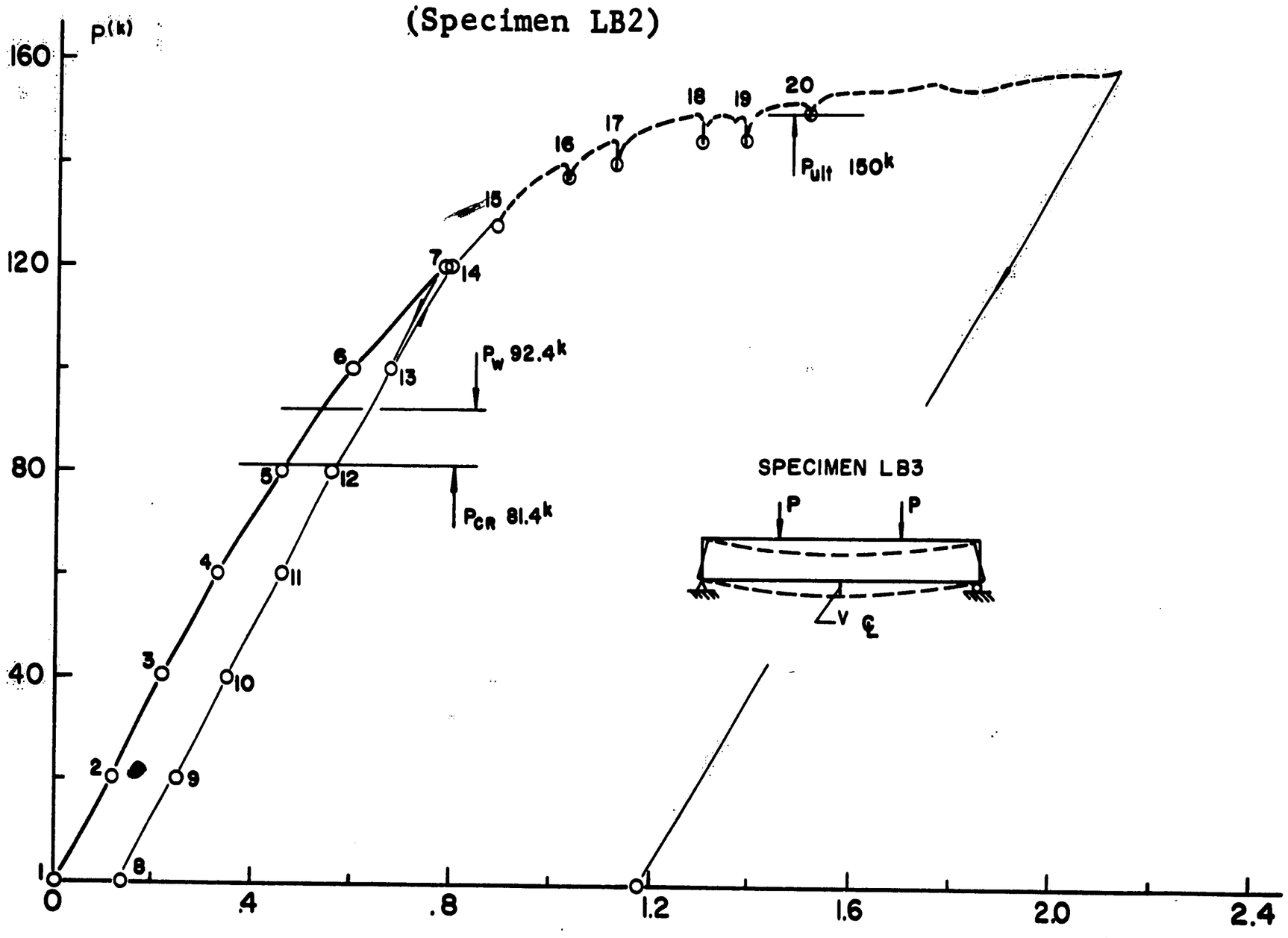

Fig. 11 Load-Vs-Centerline Deflection Curve

(Specimen LB3)

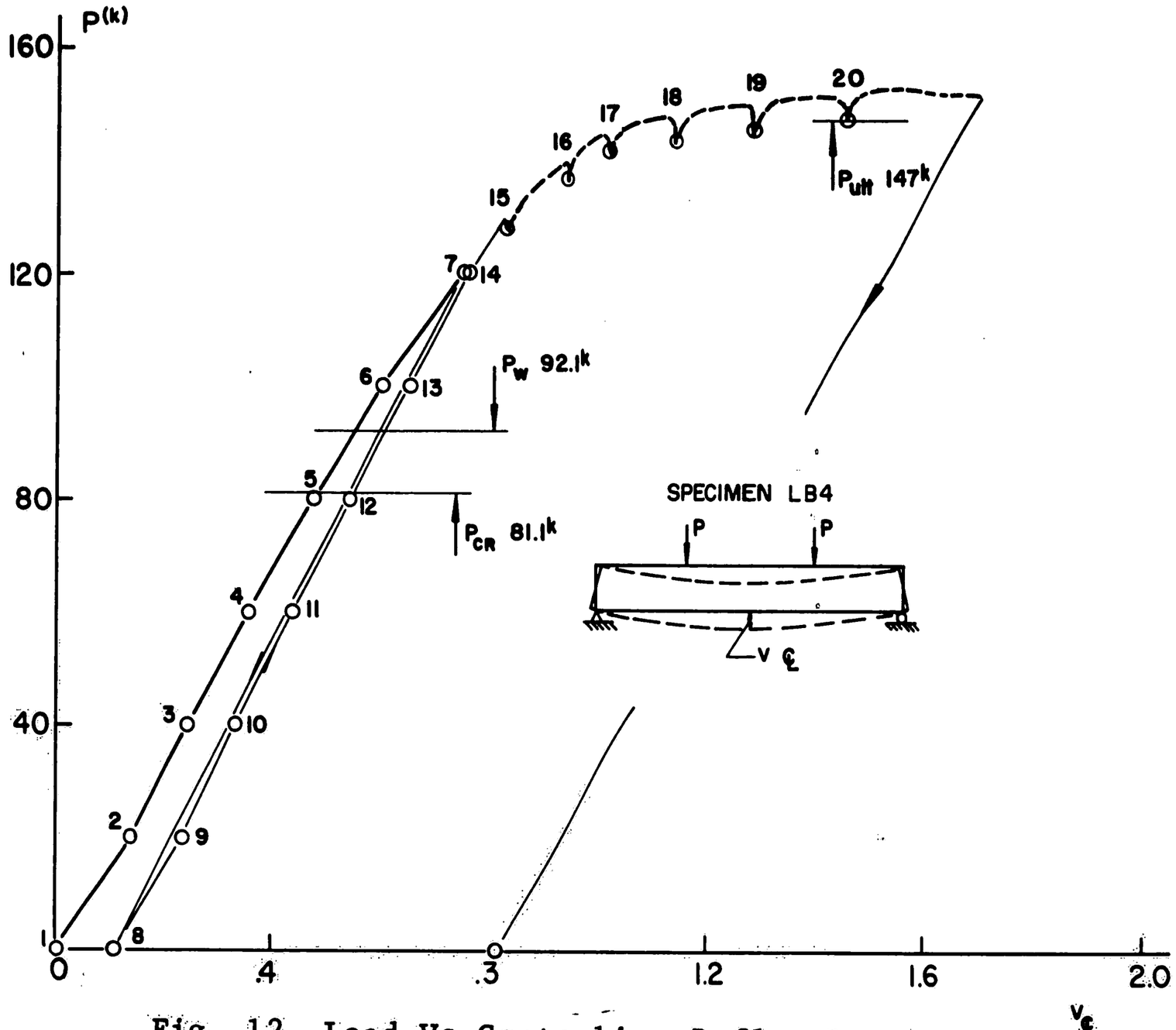

Fig. 12 Load-Vs-Centerline Deflection Curve

(Specimen LB4)

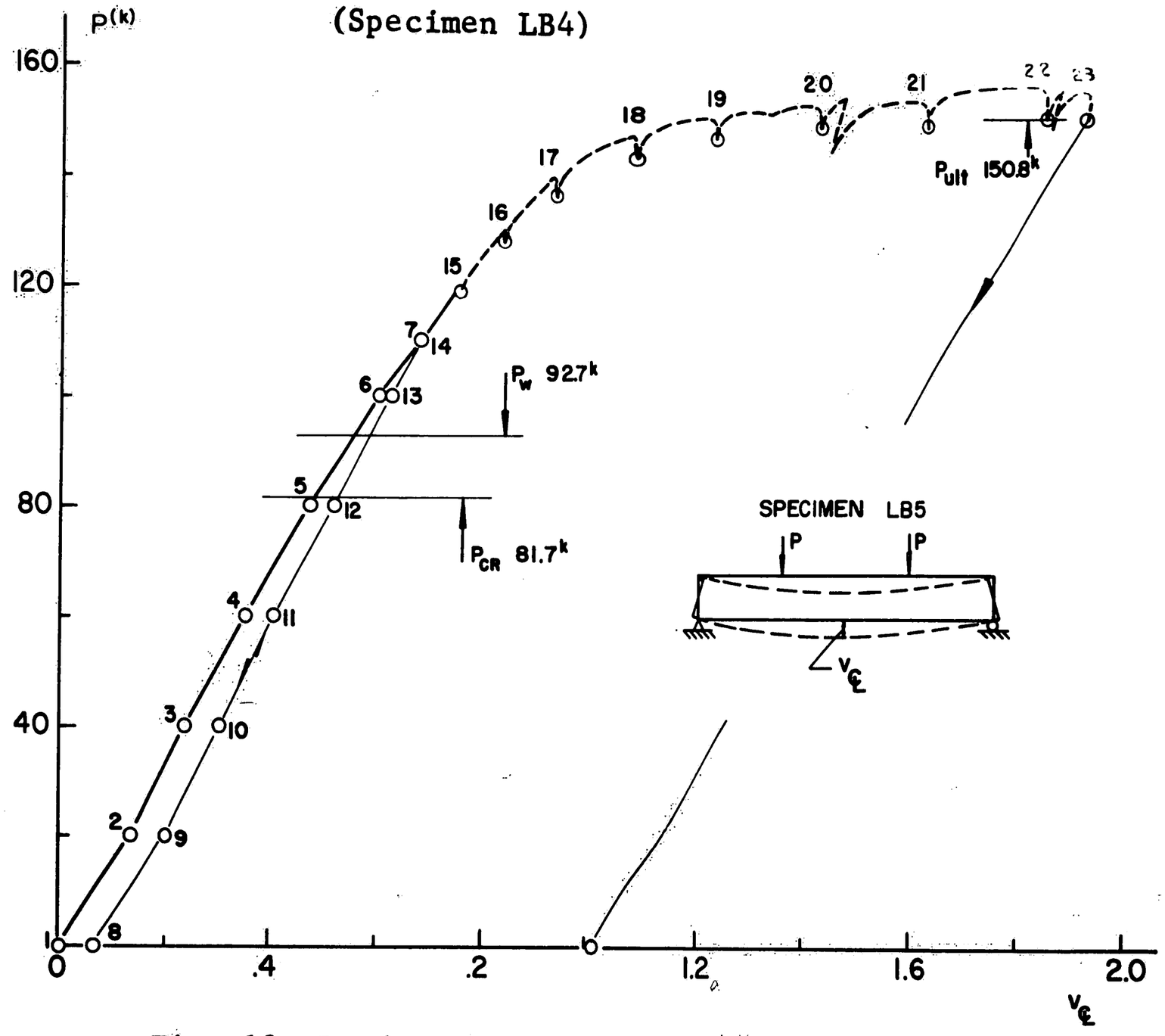

Fig. 13 Load-Vs-Centerline Deflection Curve

(Specimen LB5)

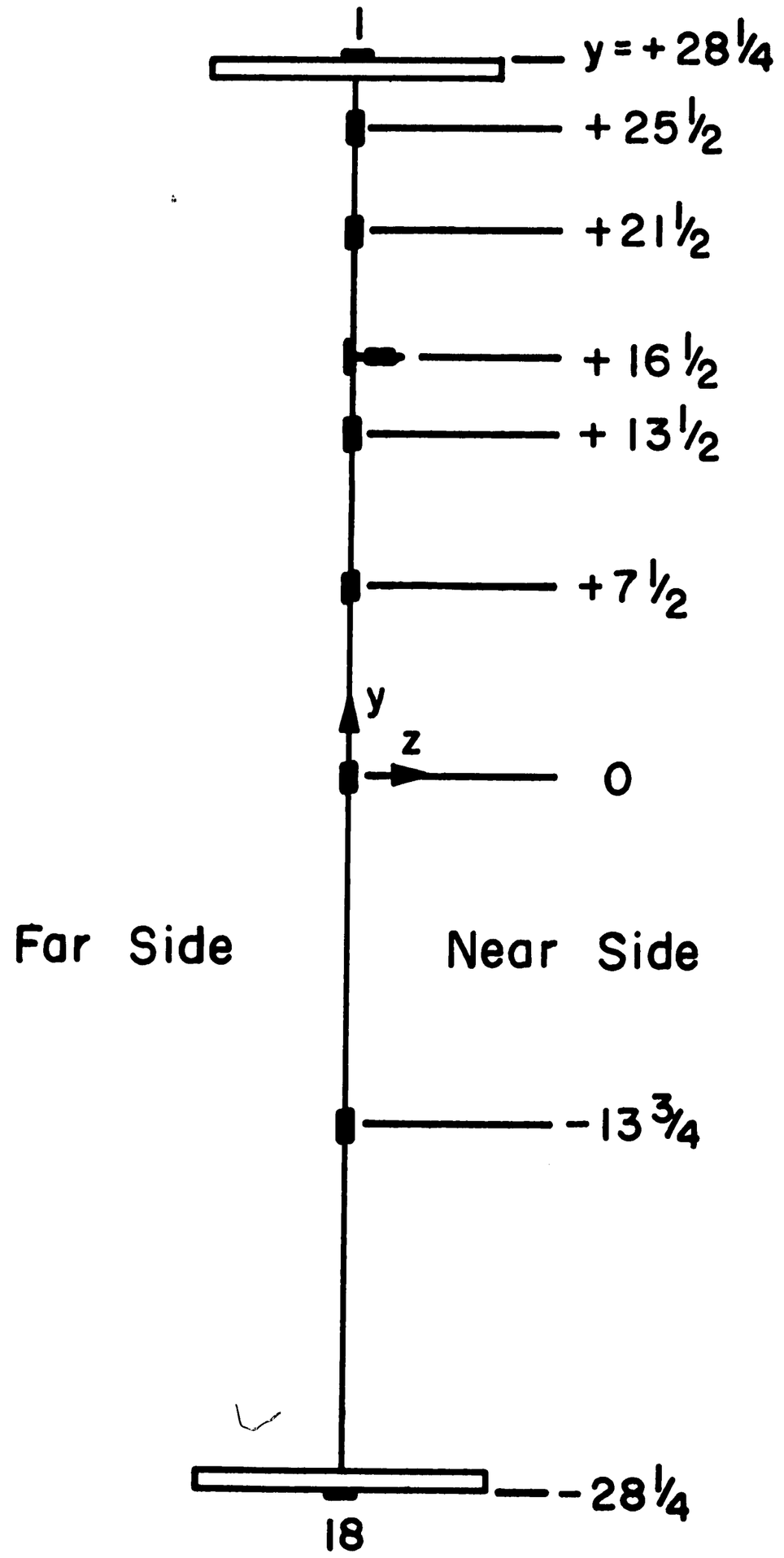

Fig. 14 Location of Strain Gages

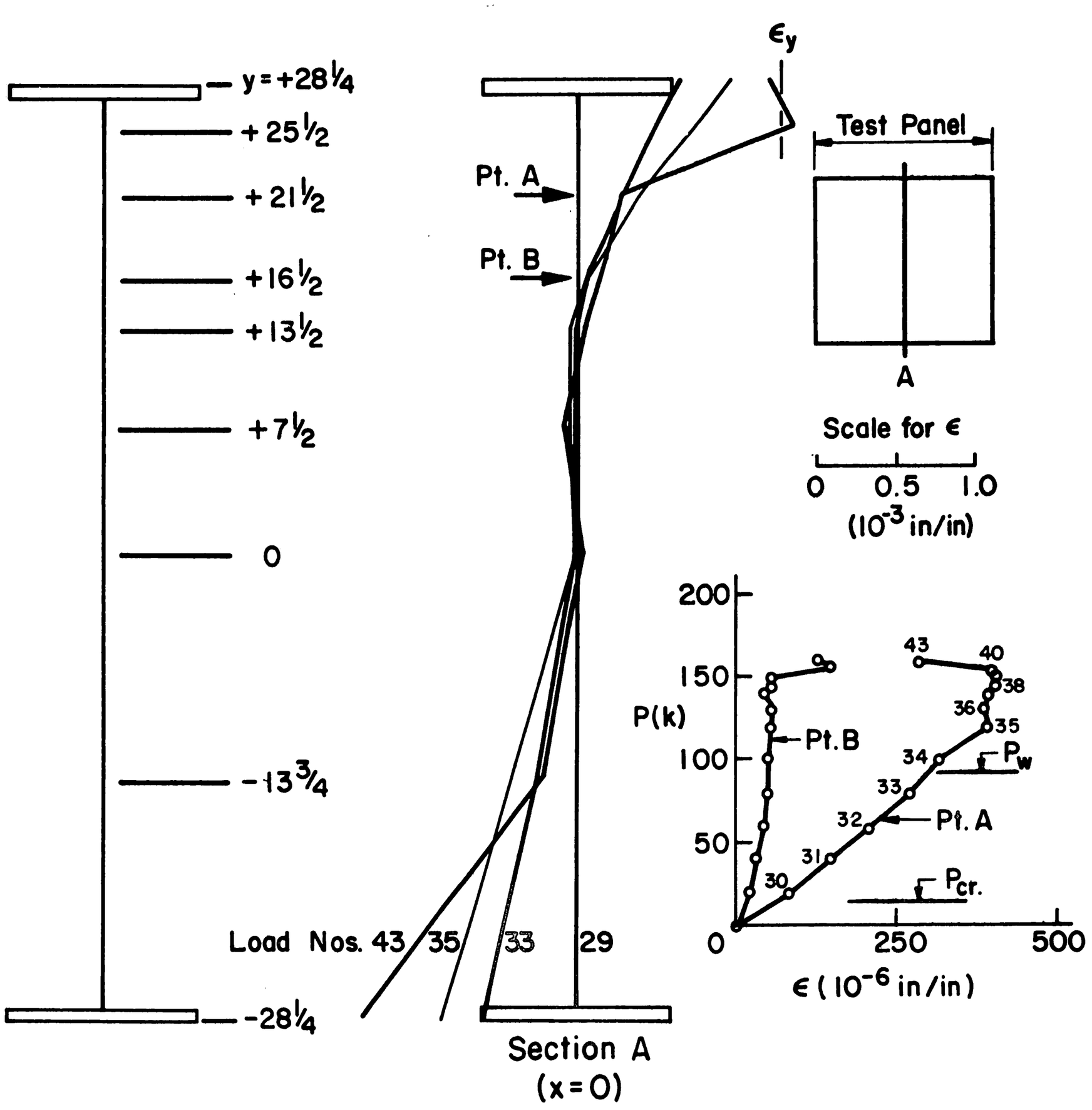

Fig. 15 Strain Distribution (Specimen LB1)

SPECIMEN LB2

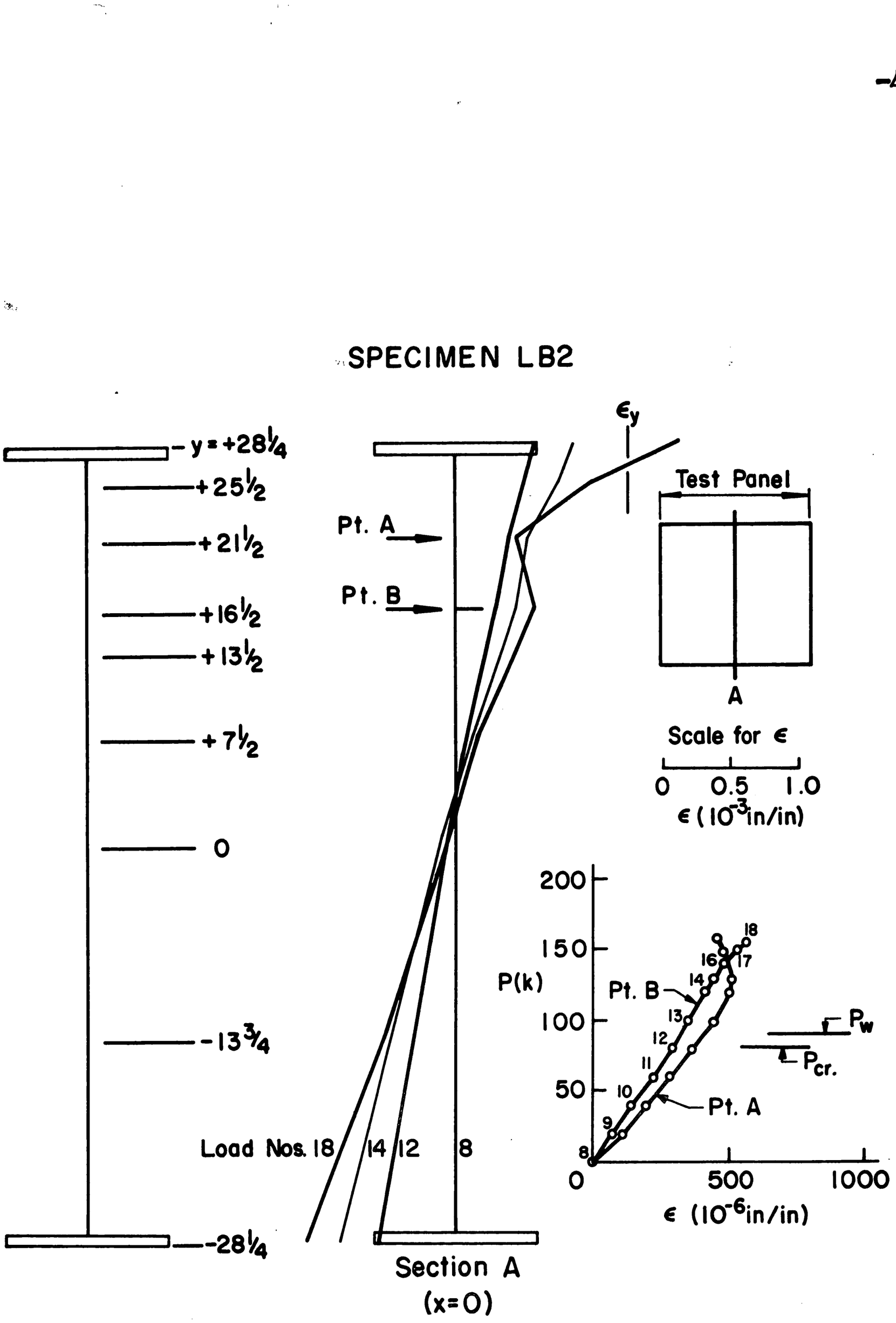

Fig. 16 Strain Distribution (Specimen LB2)

SPECIMEN LB3

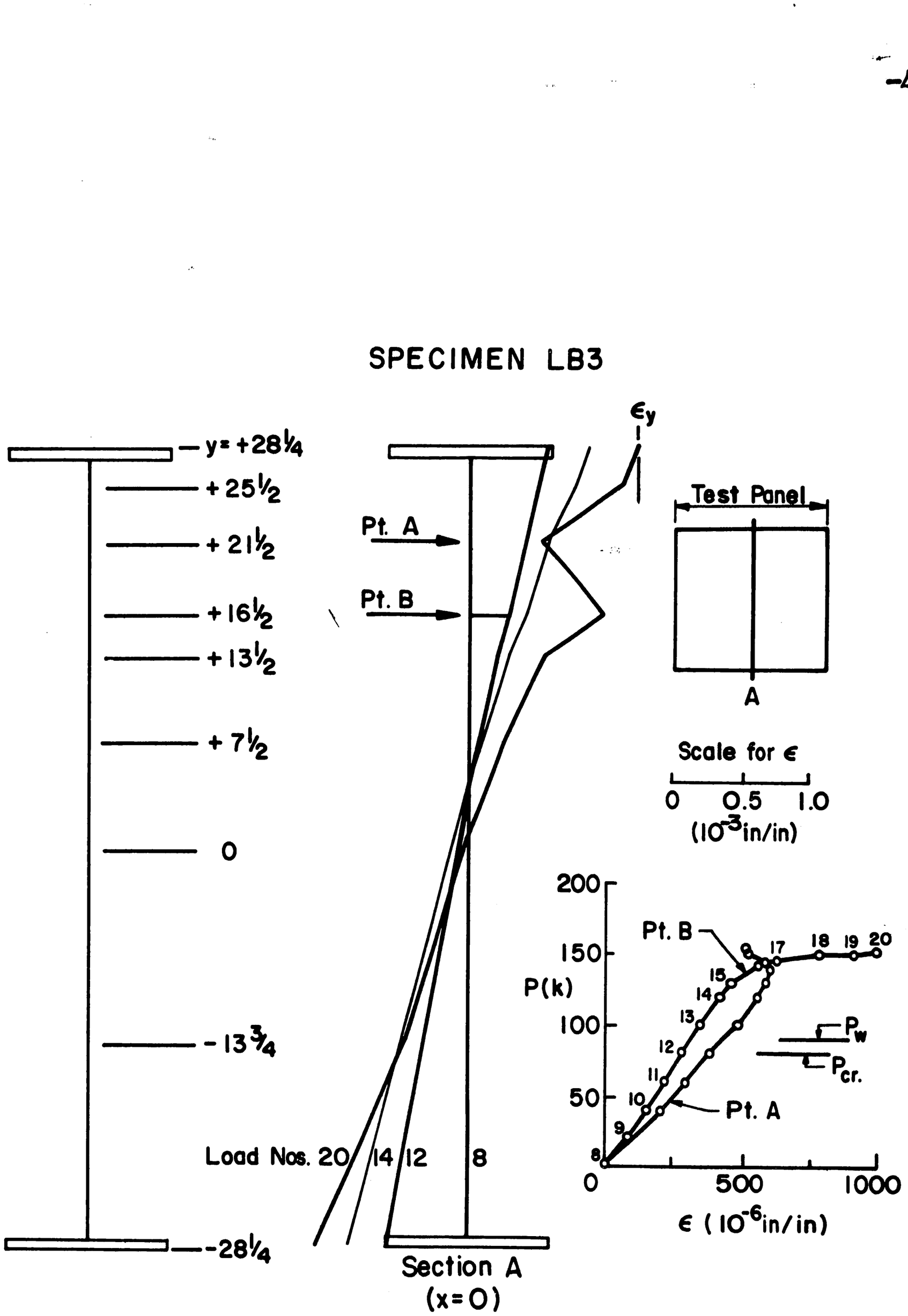

Fig. 17 Strain Distribution (Specimen LB3)

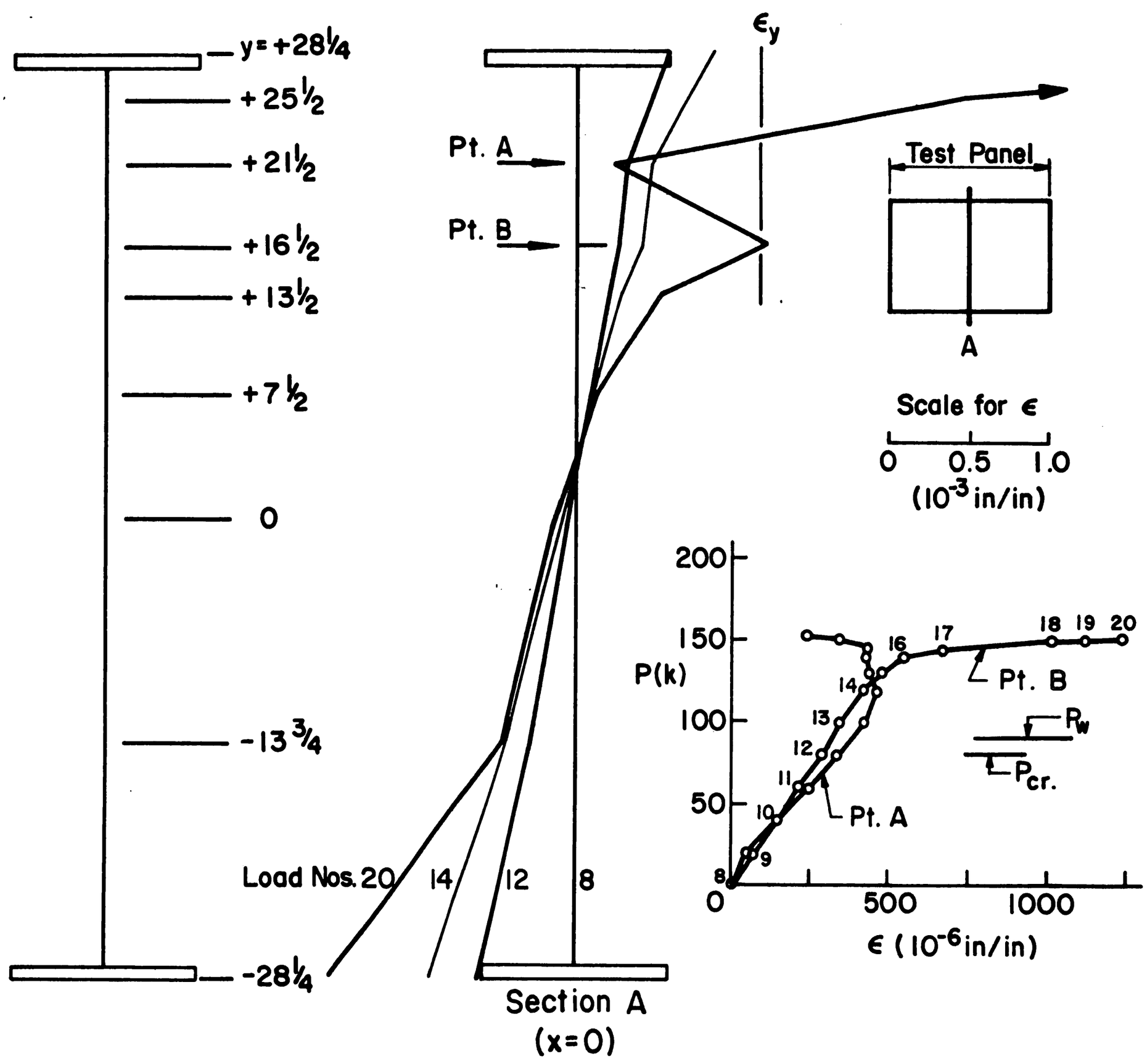

Fig. 18 Strain Distribution (Specimen LB4)

SPECIMEN LB5

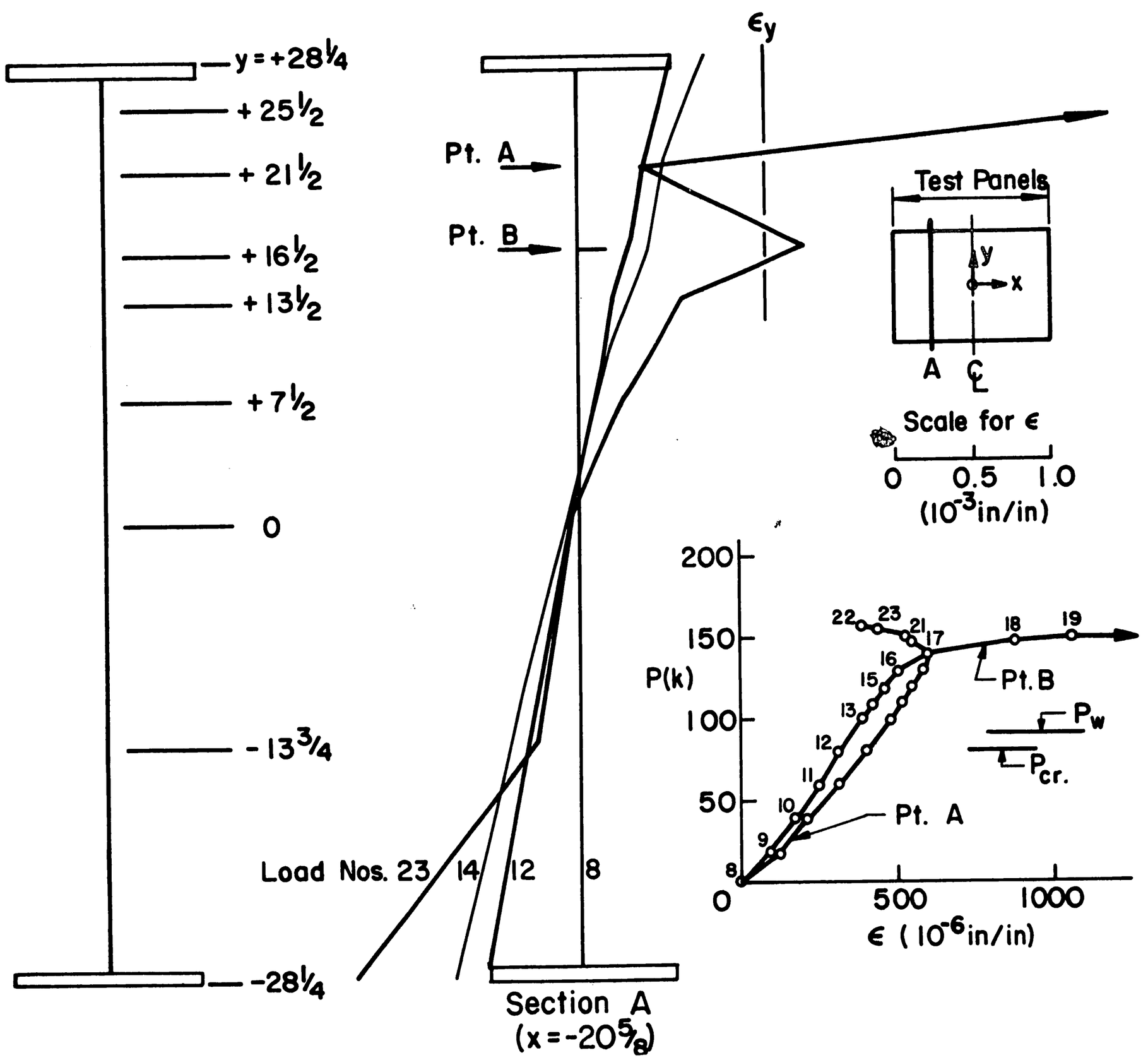

Fig. 19 Strain Distribution (Specimen LB5)

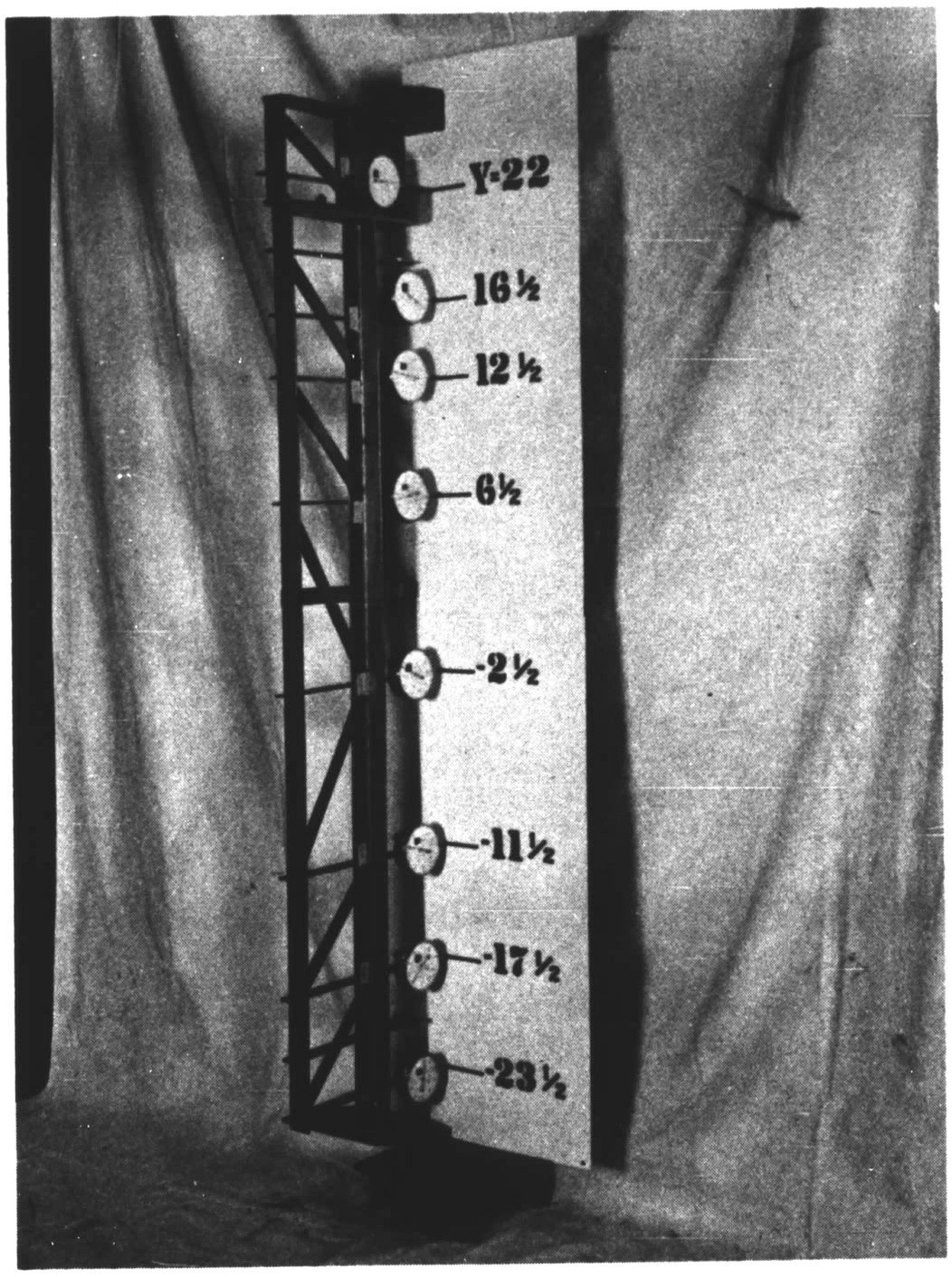

Fig. 20 Web Deflection Measuring Device

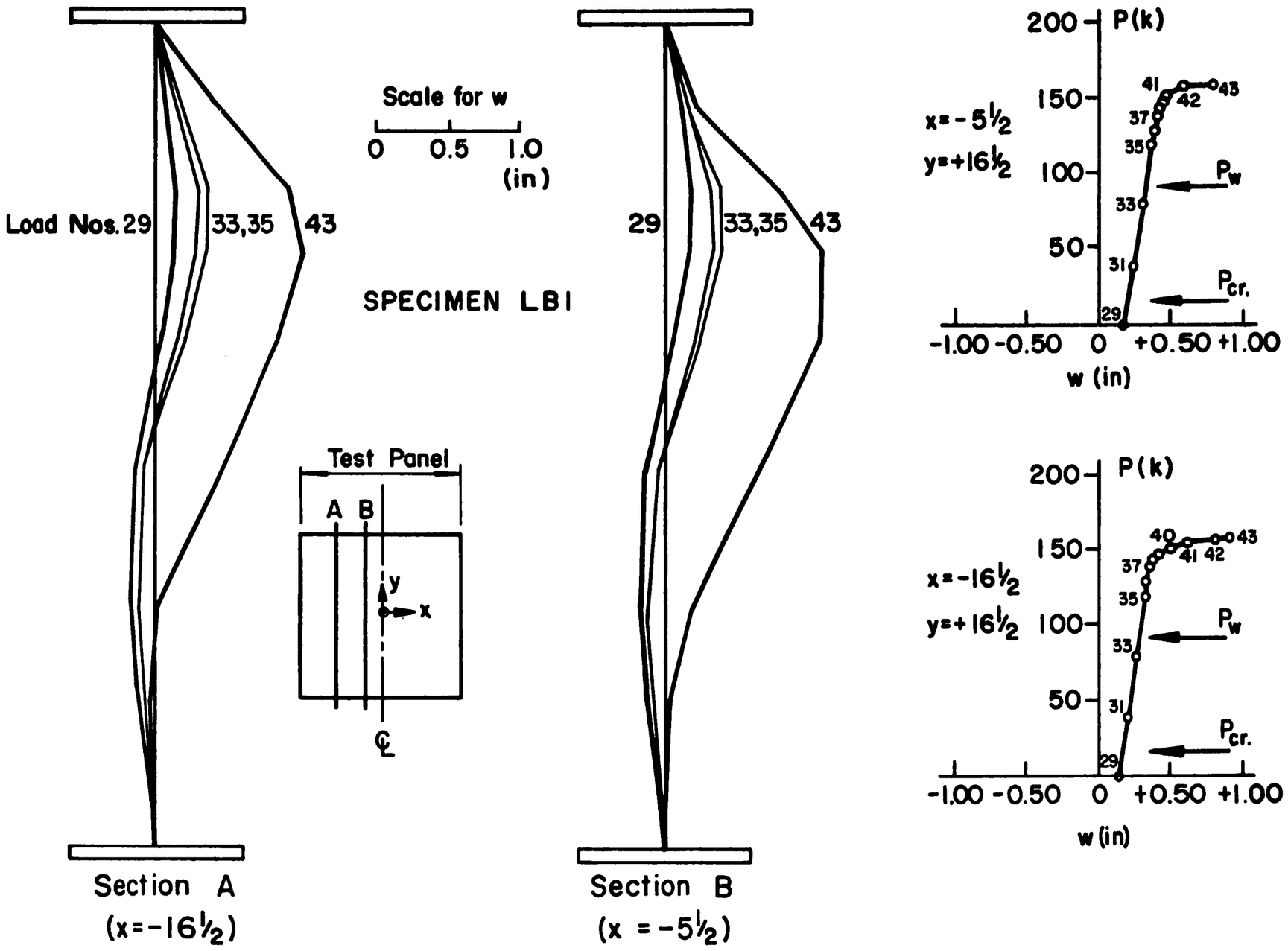

Fig. 21 Web Deflections (Specimen LB1)

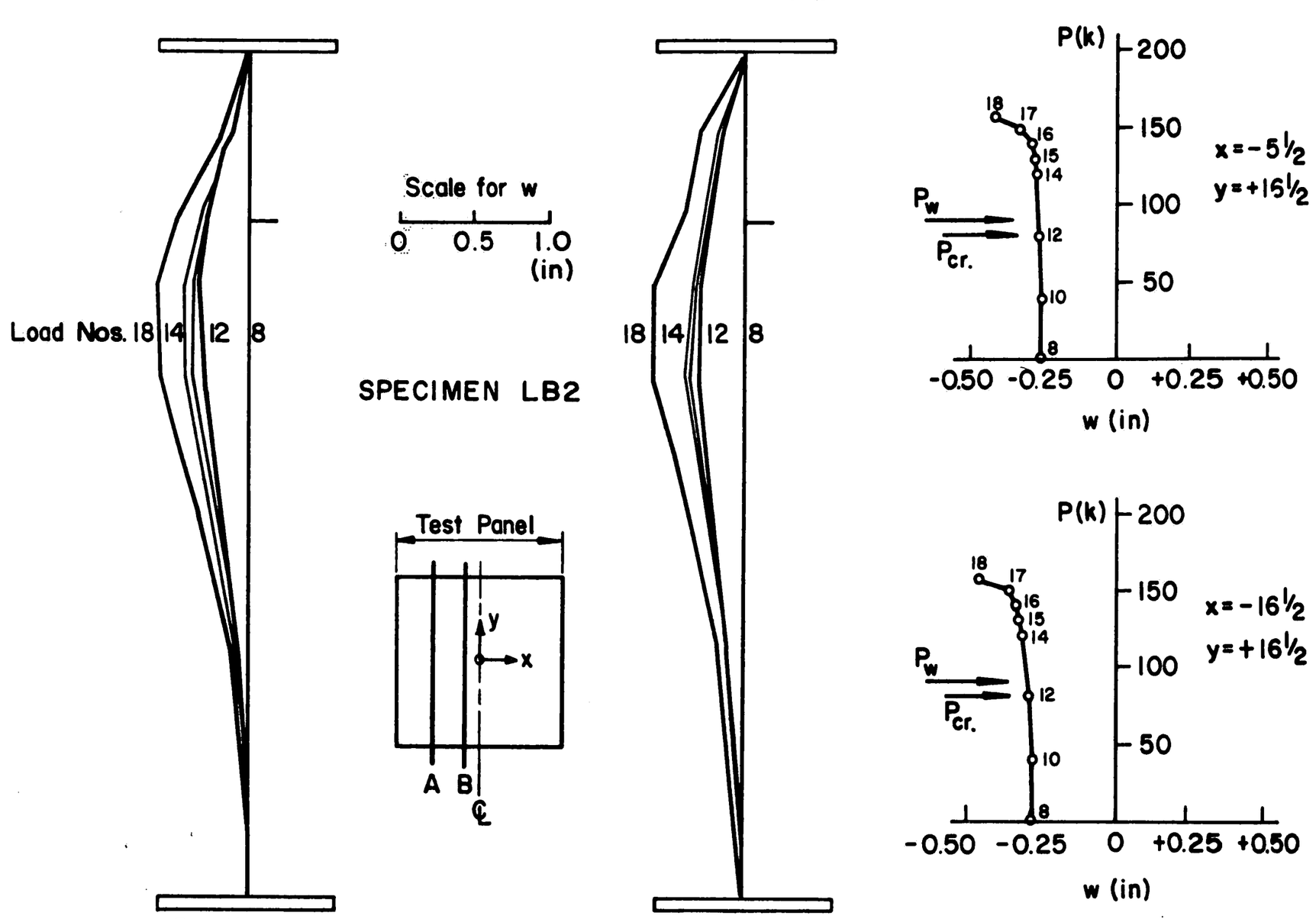

Fig. 22 Web Deflections (Specimen LB2)

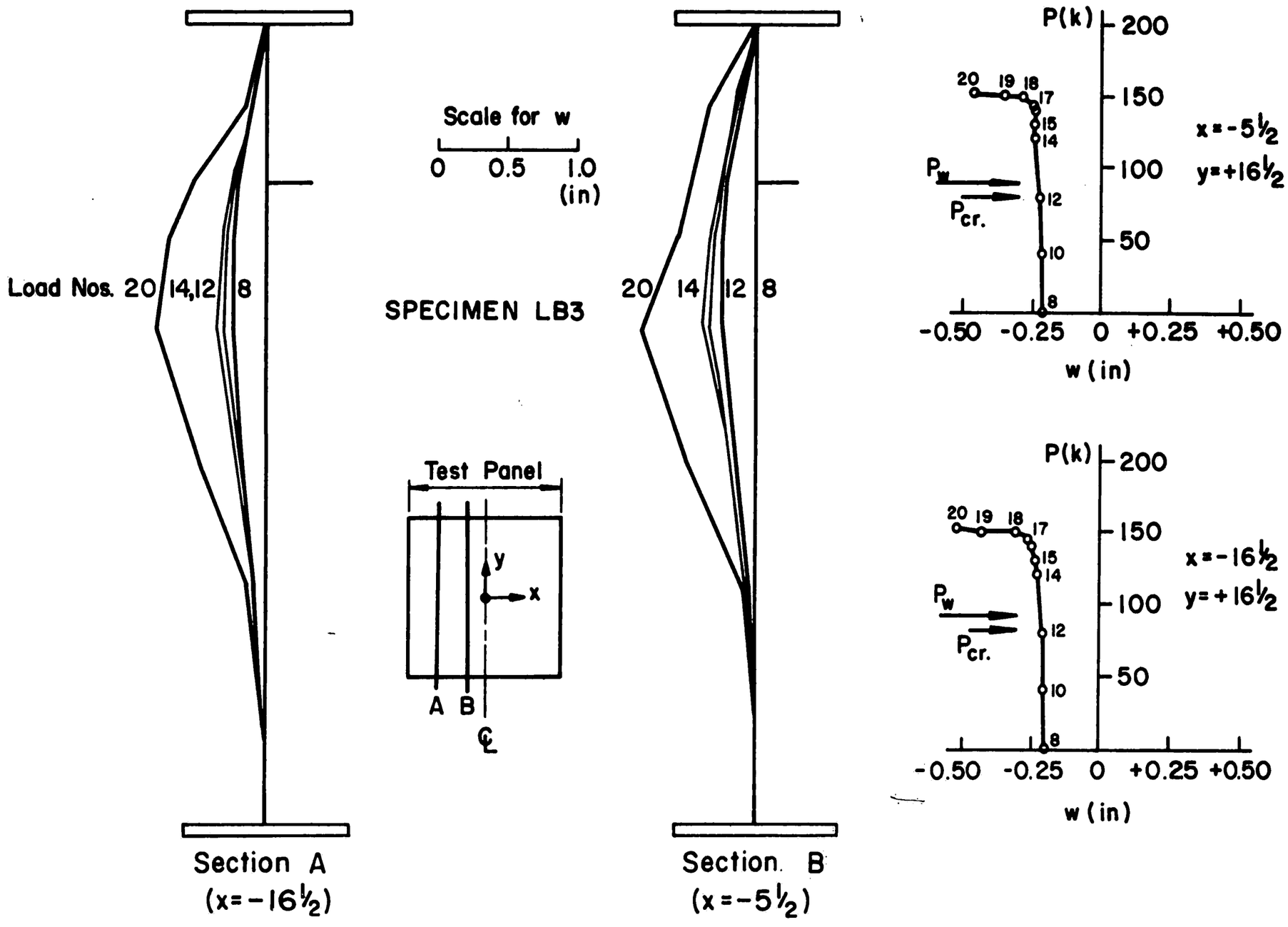

Fig. 23 Web Deflections (Specimen LB3)

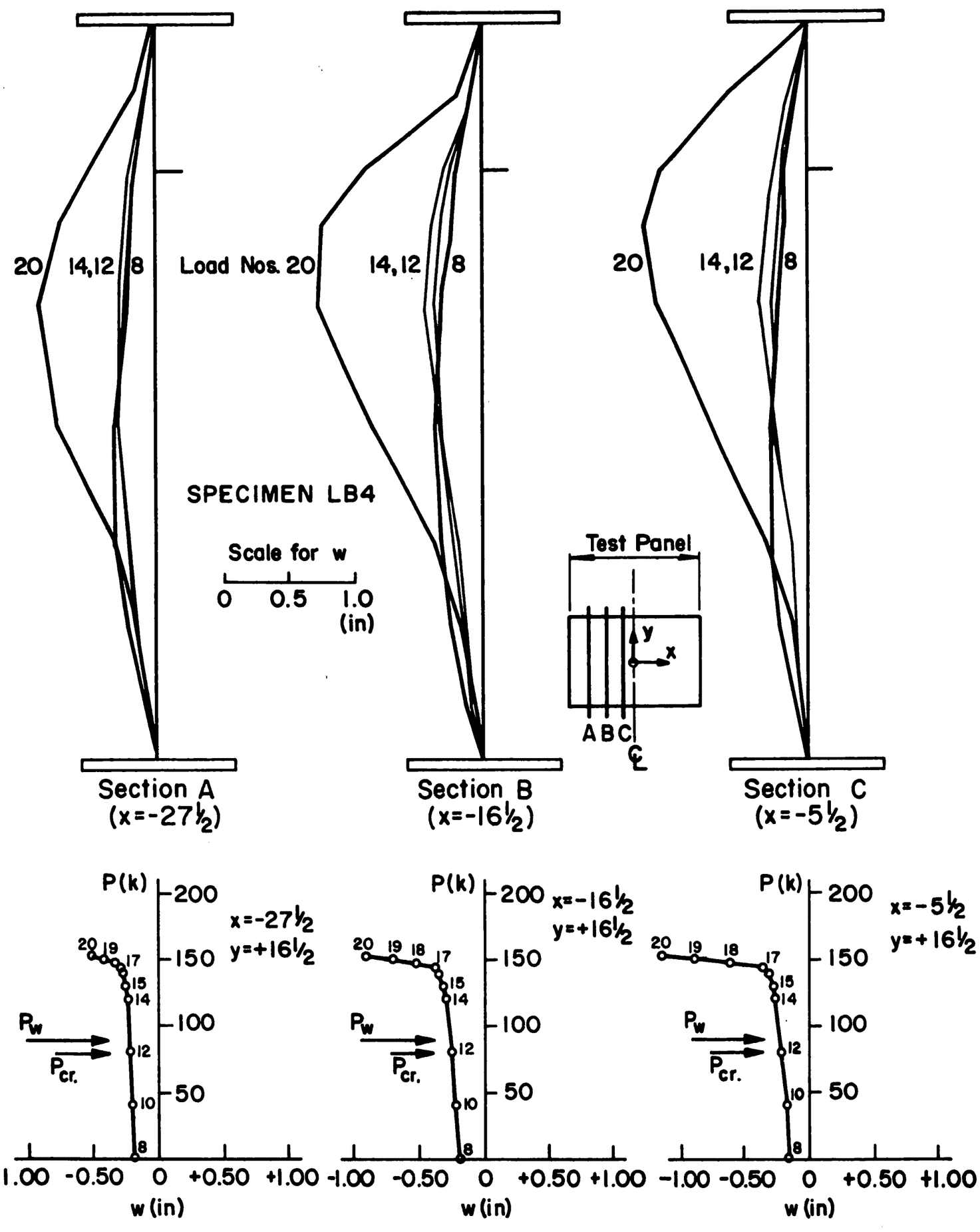

Fig. 24 Web Deflections (Specimen LB4)

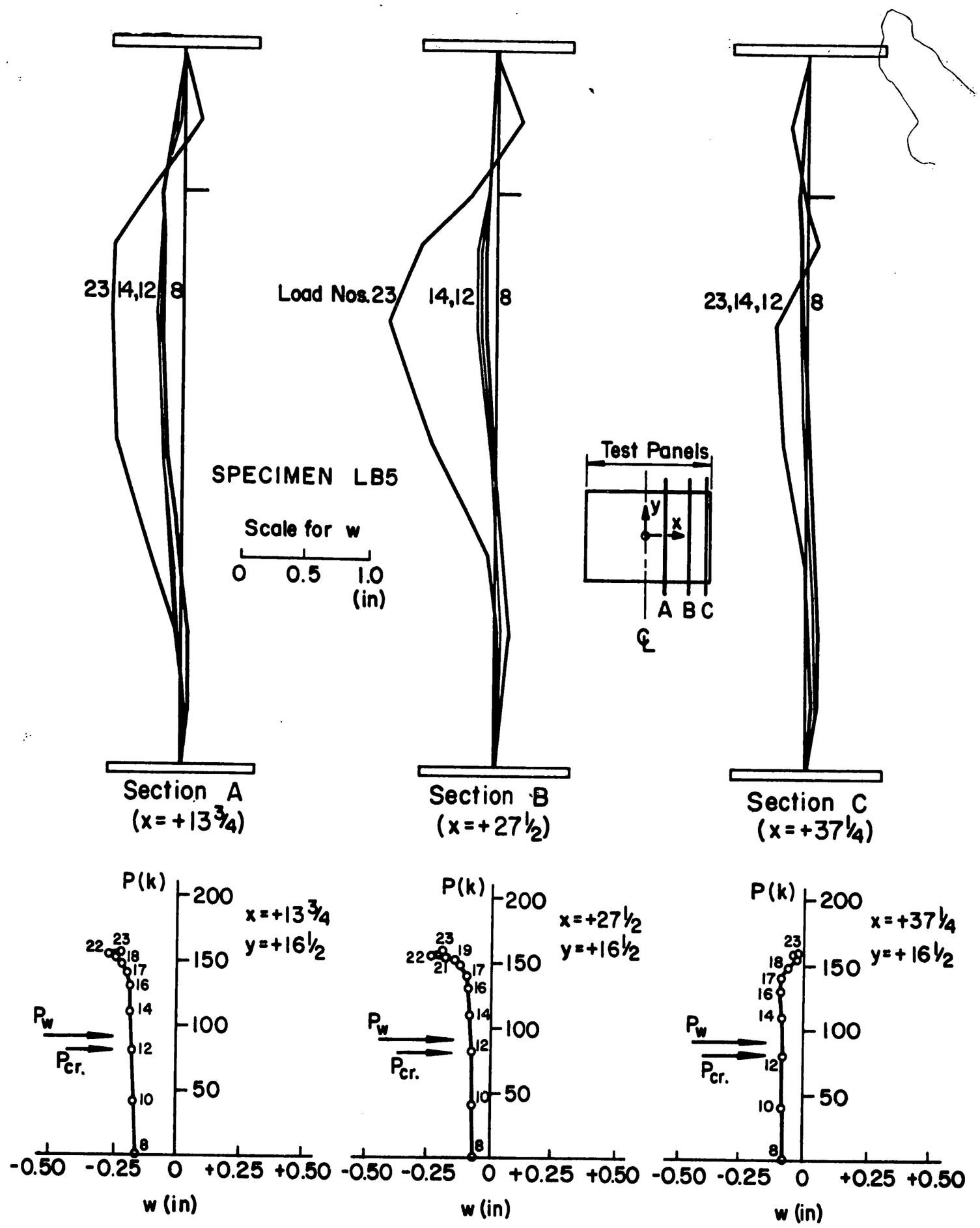

Fig. 25 Web Deflections (Specimen LB5)

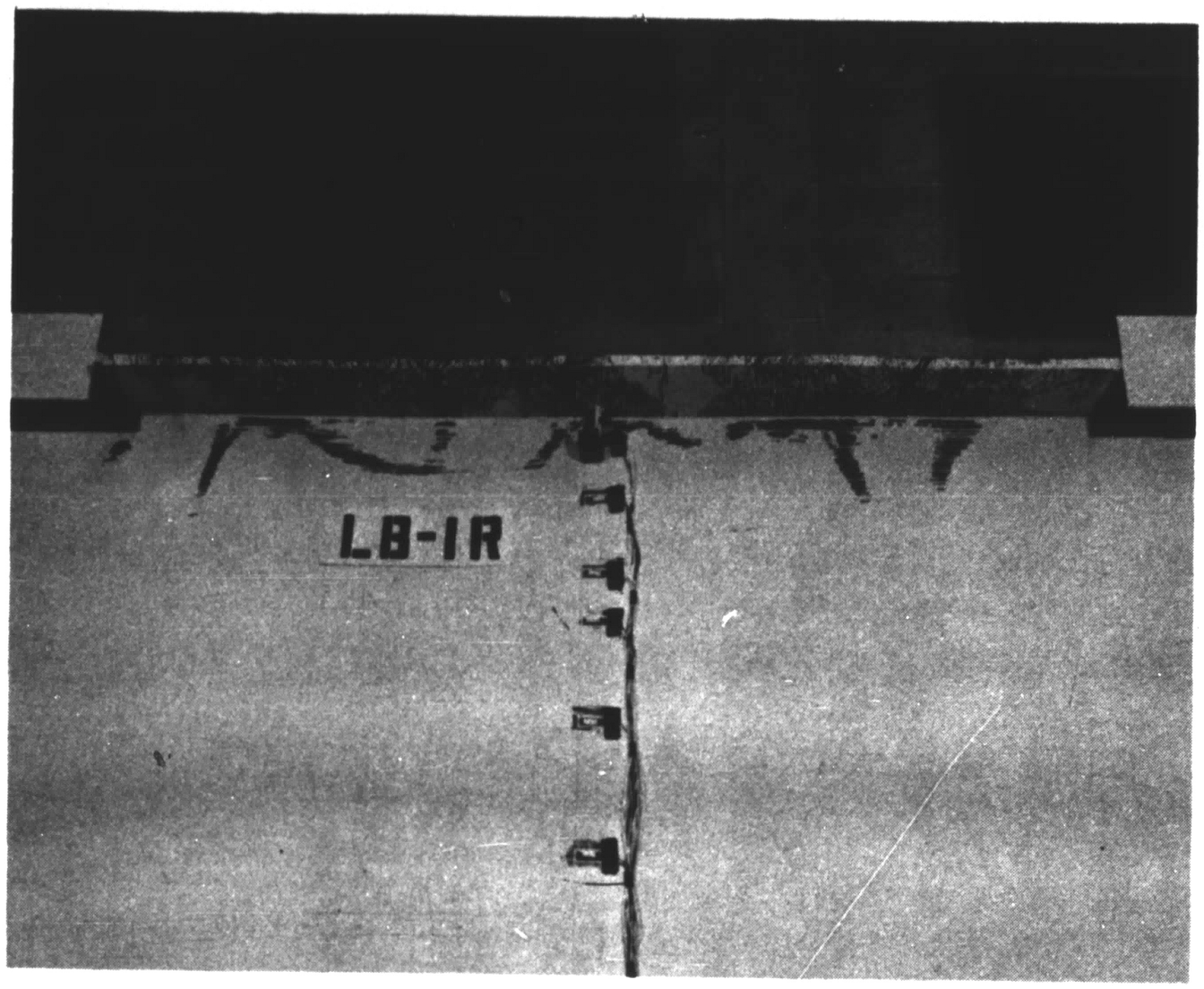

Fig. 26 Yield Pattern in Compression Flange and Web, Near Side (Specimen LB1)

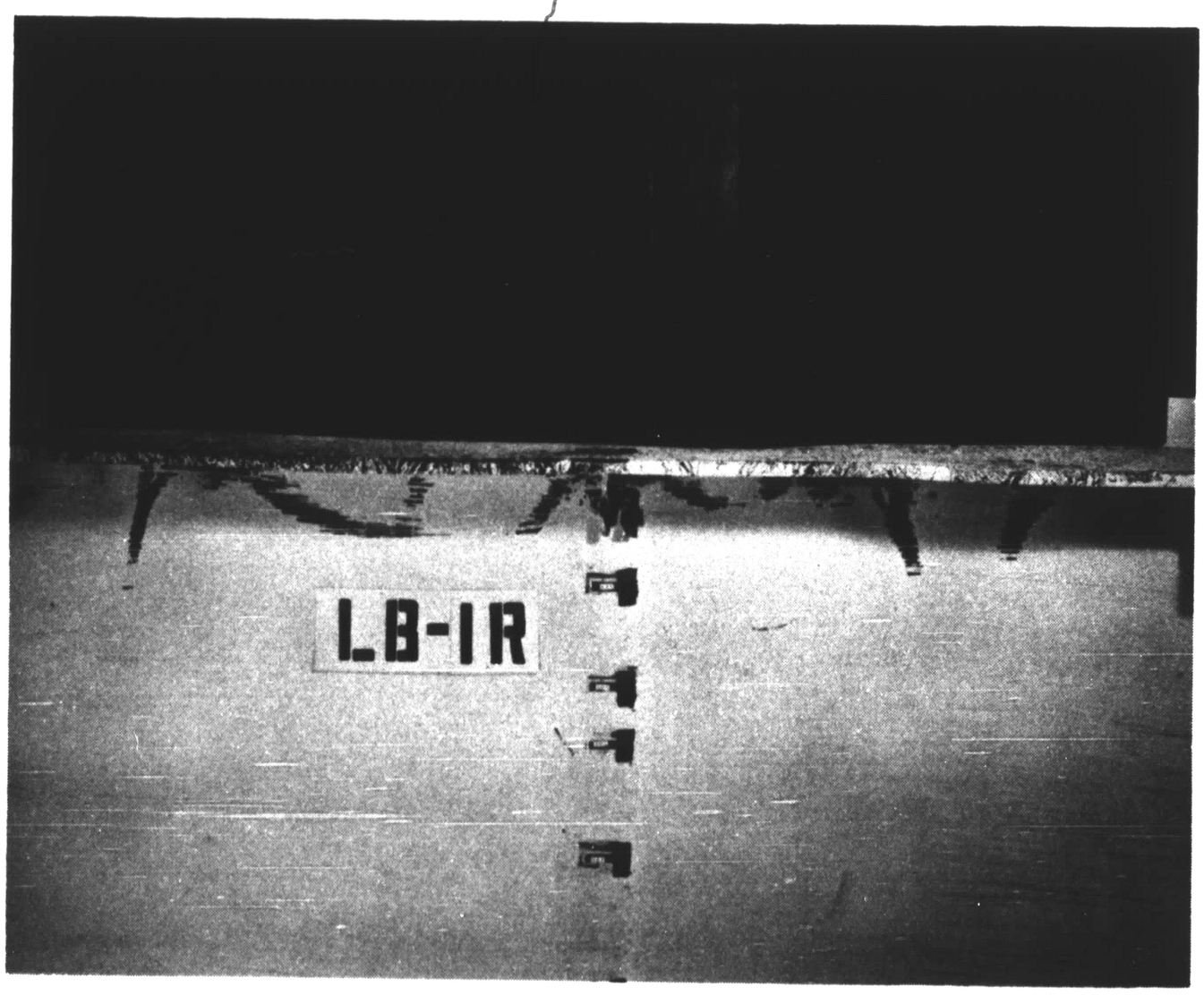

Fig. 27 Edge View of Compression Flange, Near Side (Specimen LB1)

Fig. 28 Yield Pattern on Top Surface of Compression Flange (Specimen LB1)

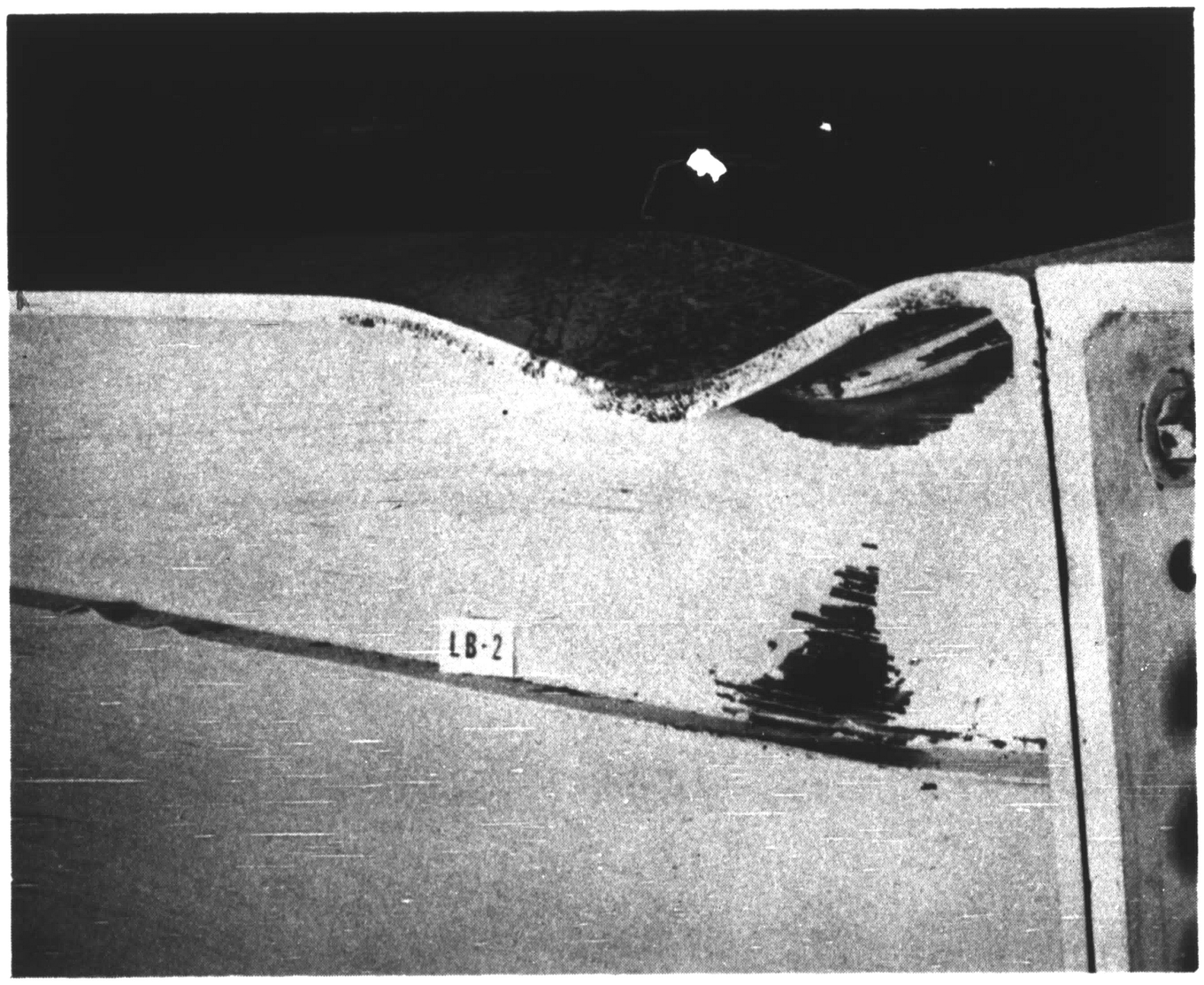

Fig. 29 Vertical Buckle, Near Side (Specimen LB2)

Fig. 30 Yielding in Side Panel, Near Side

(Specimen LB2)

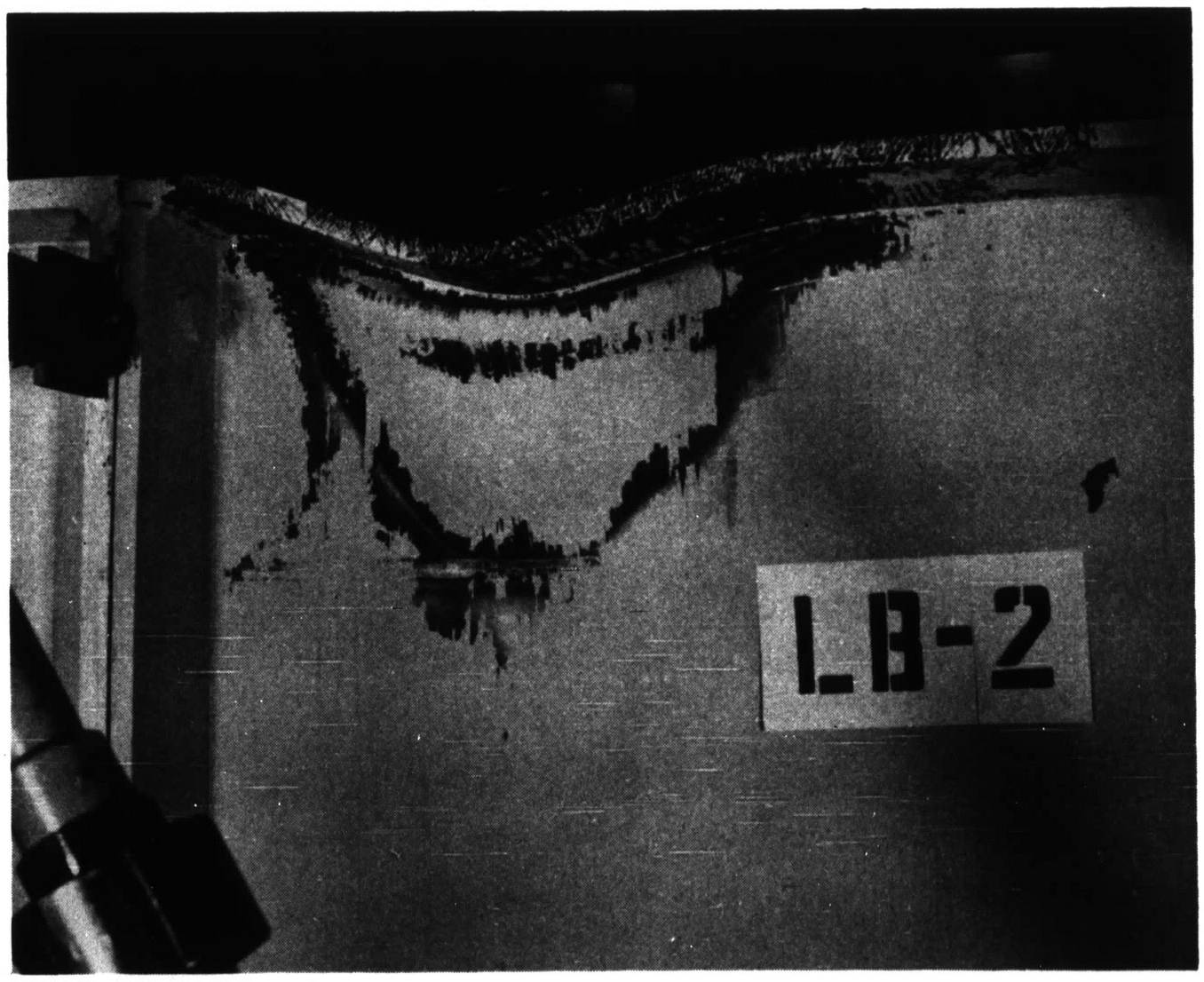

Fig. 31 Vertical Buckle, Far Side (Specimen LB2)

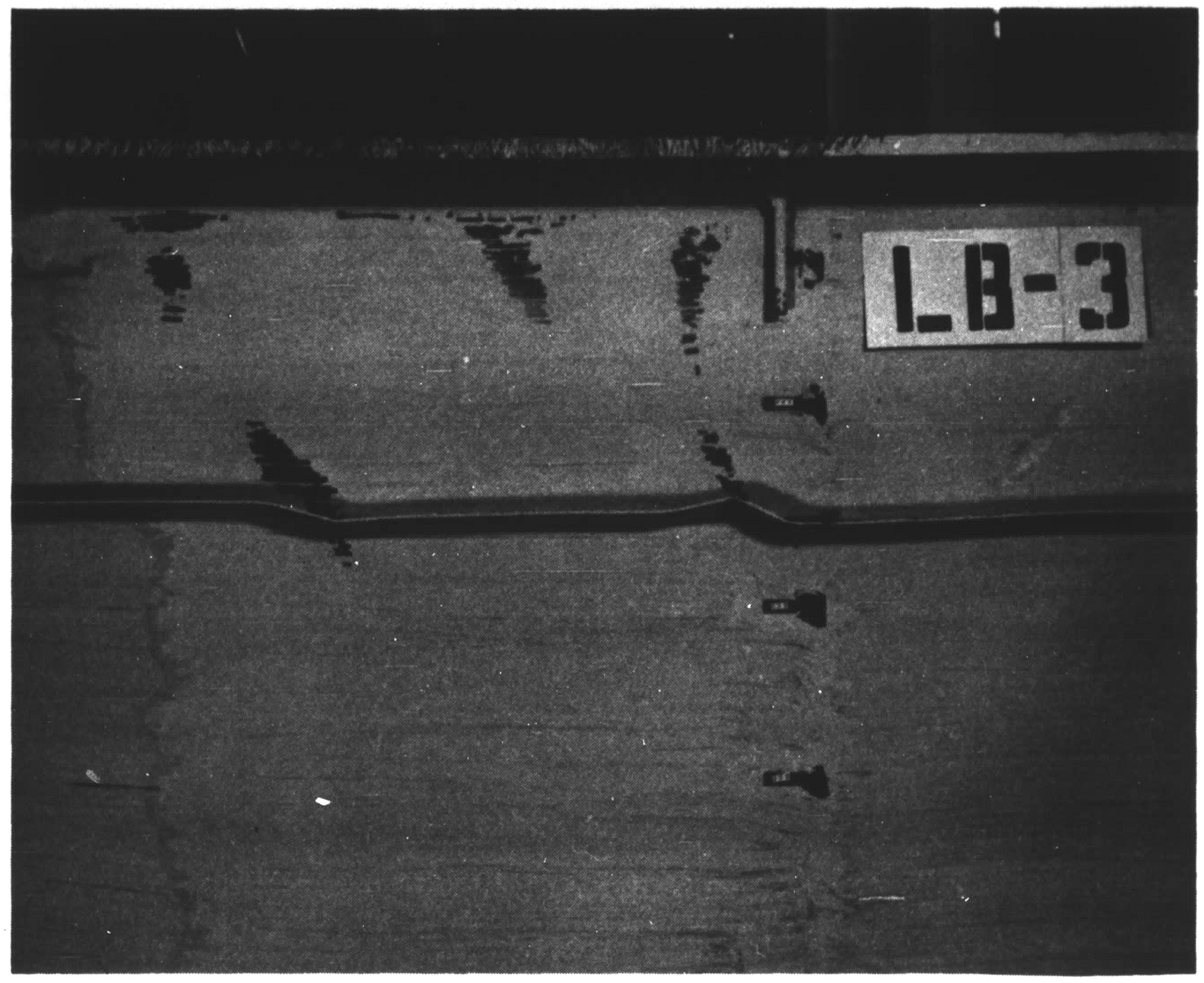

Fig. 32 Yield Pattern and Longitudinal Stiffener Buckles, Near Side (Specimen LB3)

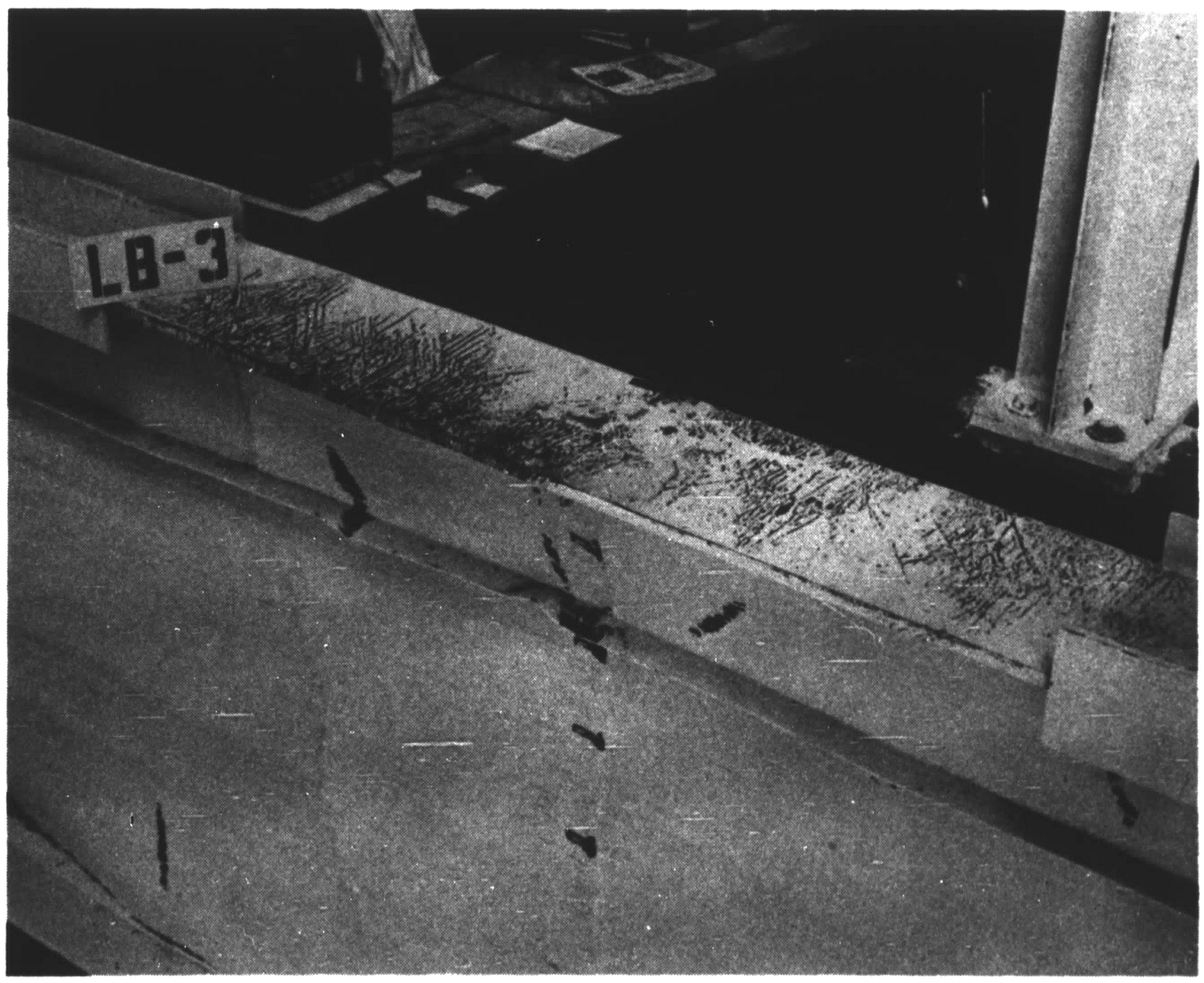

Fig. 33 Compression Flange Yield Pattern (Specimen LB3)

Fig. 34 Yield Pattern on Top Surface of Compression Flange (Specimen LB3)

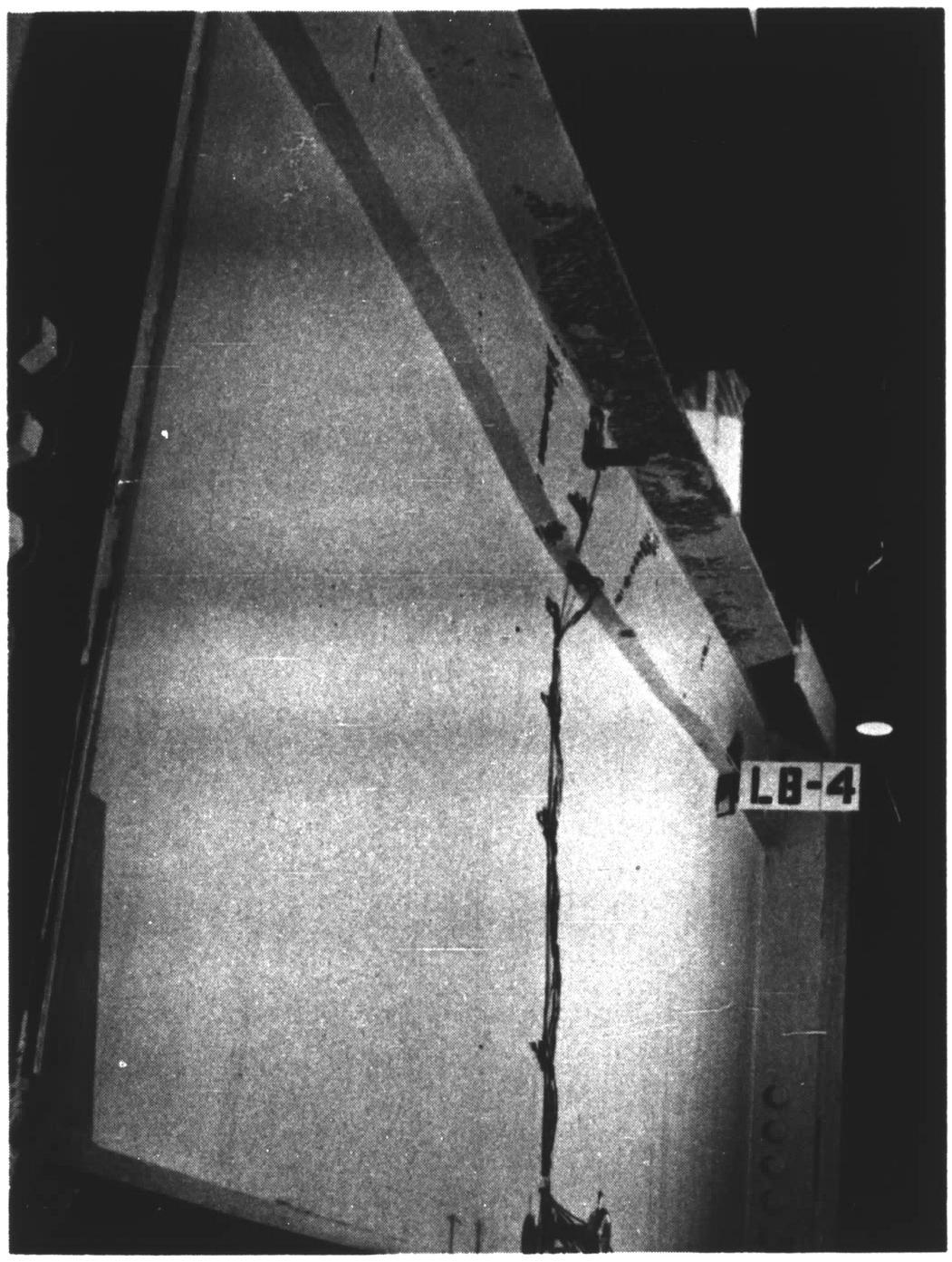

Fig. 35 Test Panel After Ultimate Load, Near Side

(Specimen LB4)

Fig. 36 Compression Flange Yield Pattern After Ultimate Load (Specimen LB4)

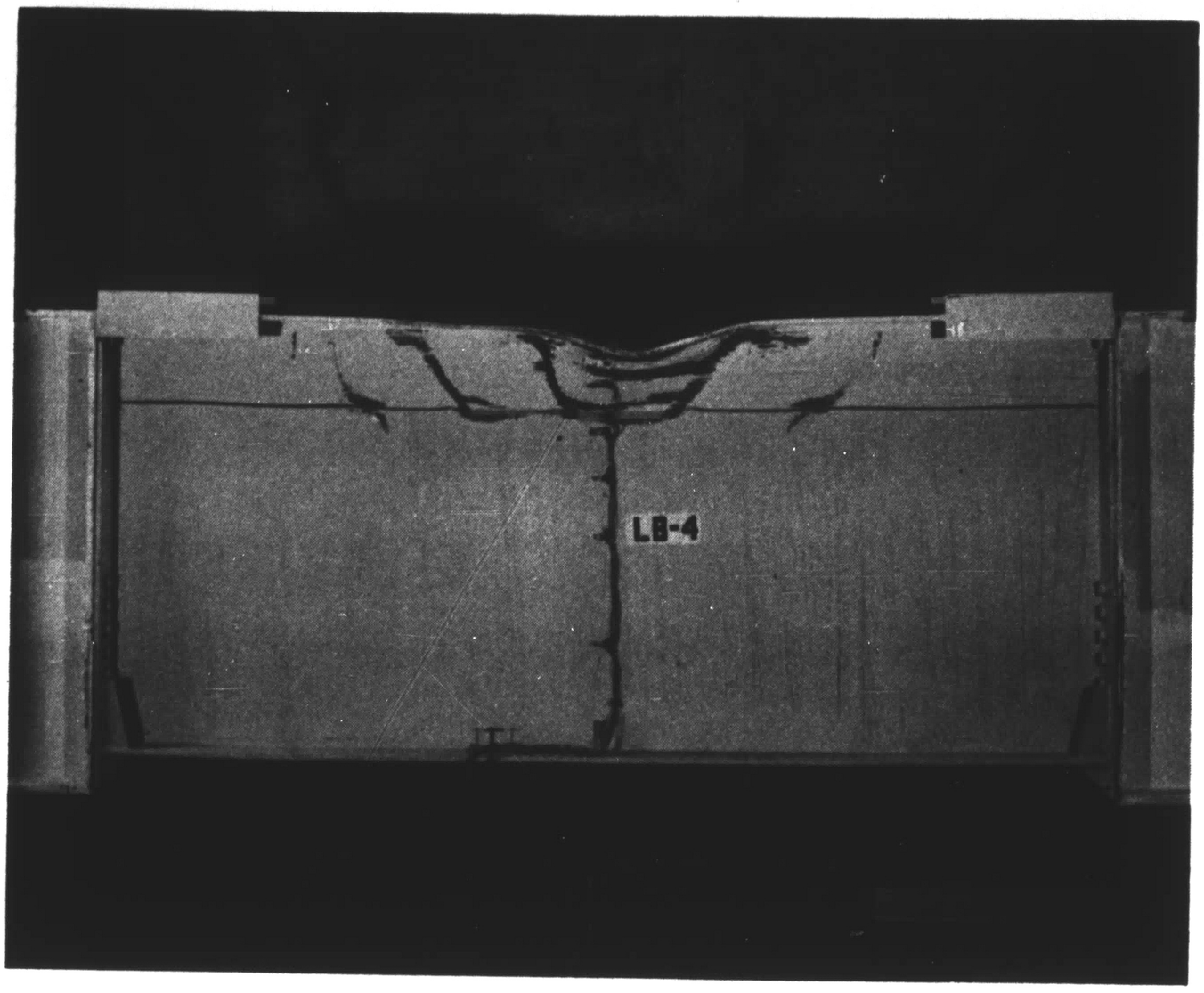

Fig. 37 Failure Due to Vertical Buckling, Near Side (Specimen LB4)

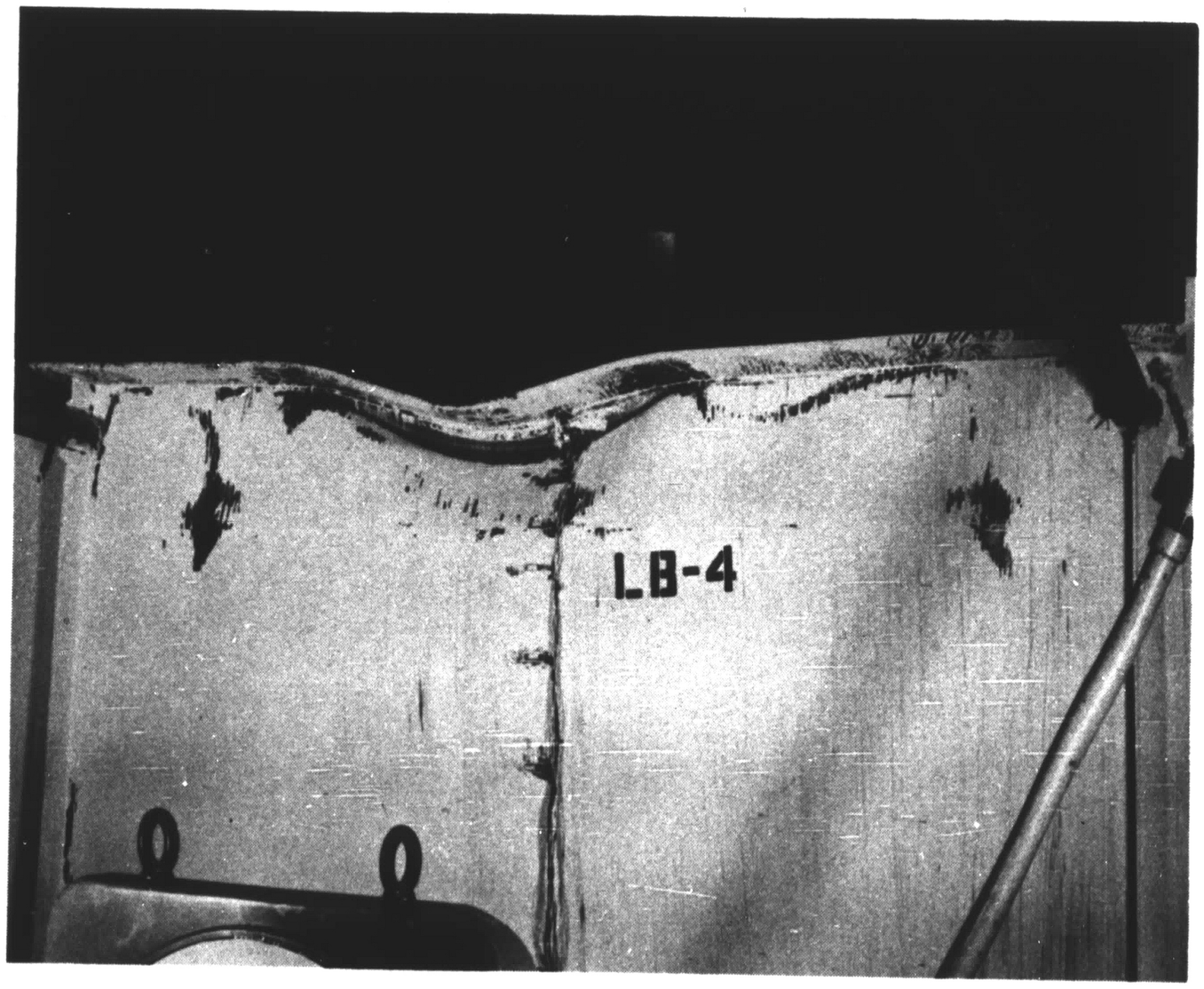

Fig. 38 Failure Due to Vertical Buckling, Far Side (Specimen LB4)

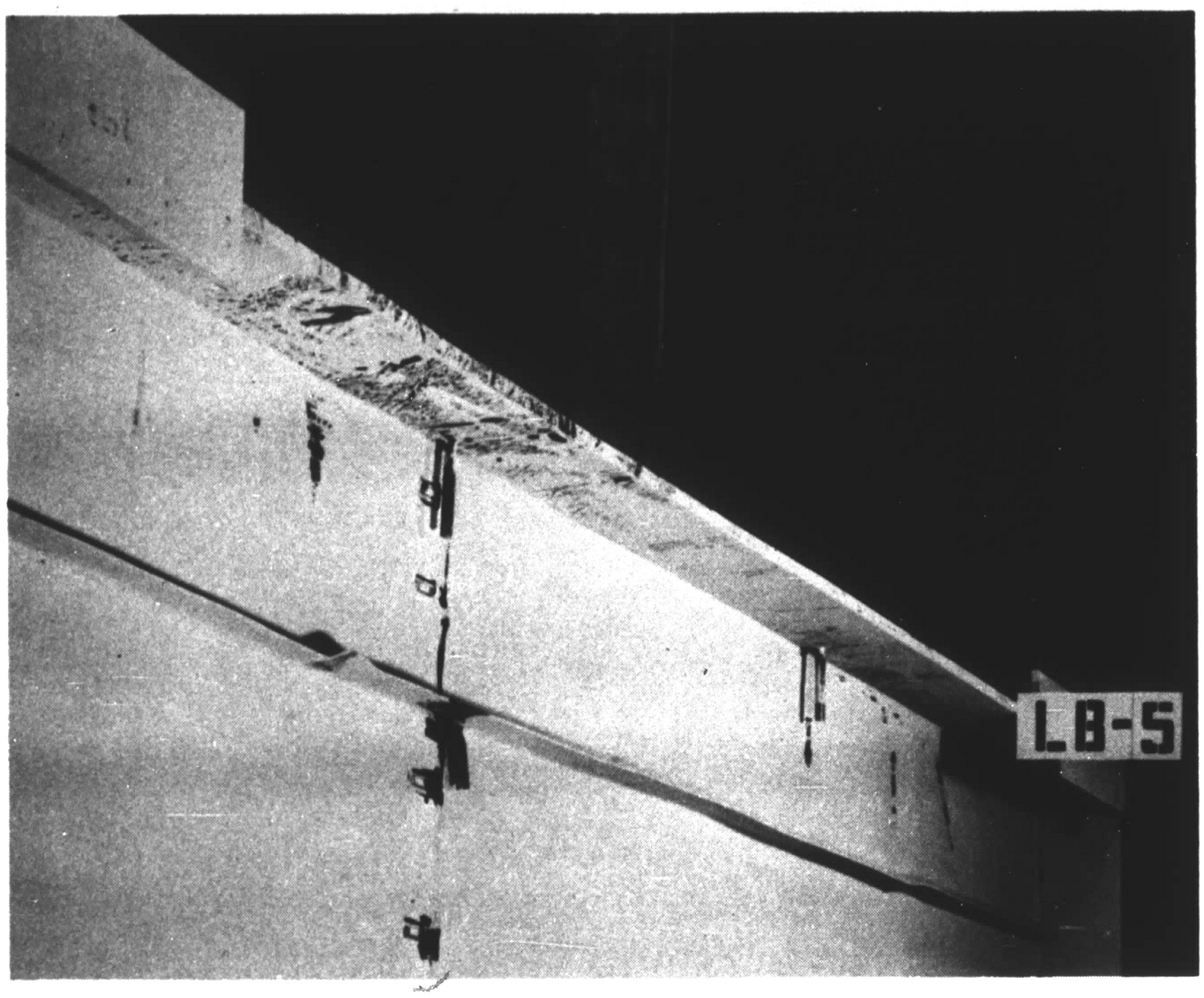

Fig. 39 Yield Pattern and Horizontal Stiffener Buckles, Near Side (Specimen LB5)

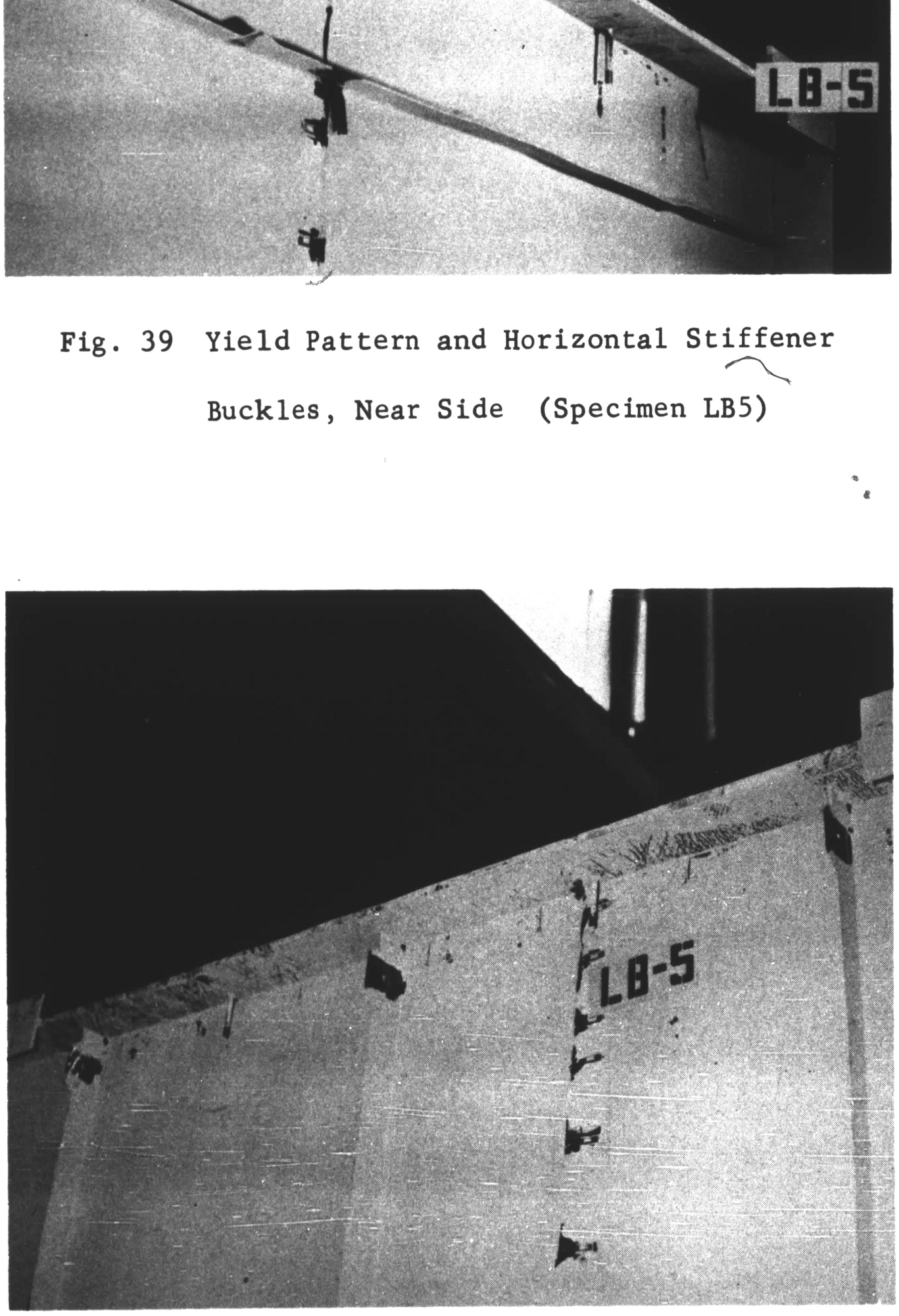

Fig. 40 Yield Pattern, Far Side (Specimen LB5)

Fig. 41 Compression Flange Yield Pattern

(Specimen LB5)

8. REFERENCES

1. K. Basler and B. Thürlimann
STRENGTH OF PLATE GIRDERS IN BENDING, Proc., ASCE, Vol. 87, No. ST6, August, 1961.

2. K. Basler
STRENGTH OF PLATE GIRDERS IN SHEAR, Proc., ASCE, Vol. 87, No. ST7, October, 1961

3. K. Basler
STRENGTH OF PLATE GIRDERS UNDER COMBINED BENDING AND SHEAR, Proc., ASCE, Vol. 87, No. ST7, October, 1961

4. K. Basler, B. T. Yen, J. A. Mueller and B. Thürlimann
WEB BUCKLING TESTS ON WELDED PLATE GIRDERS, Bulletin No. 64, Welding Research Council, New York, Sept., 1960

5. American Institute of Steel Construction, Inc.
MANUAL OF STEEL CONSTRUCTION, 6th Edition, 1963

6. American Association of State Highway Officials
STANDARD SPECIFICATIONS FOR HIGHWAY BRIDGES, 1961

7. Deuscher Normenausschuss
DIN 4114 (German Buckling Specifications), Blatt 1 und 2, Beuth-Vertrieb GmbH, Berlin and Cologne, July 1952

8. British Standards Institution
BRITISH STANDARD 153 : STEEL GIRDER BRIDGES, Parts 3B and 4, British Standards House, London, 1958

9. F. Stussi, C. Dubas and P. Dubas
LE VOILEMENT DE L'ÂME DES POUTRES FLÉCHIES, AVEC RAIDISSUER AU CINQUIÈME SUPÉRIEUR, Pub. IABSE, Vol. 17, 1957, p. 217
(THE BUCKLING DUE TO BENDING OF WEBS OF BEAMS HAVING STIFFENERS IN THE TOP FIFTH OF THE WEB)

10. K. Basler
FURTHER TESTS ON WELDED PLATE GIRDERS, Proc., AISC Natl. Engrg. Conf., 1960

9. VITA

The author was born on September 11, 1941 in Yonkers, New York and is the oldest son of Dominic and Antionette D'Apice. He attended Yonkers Public Schools and graduated from Yonkers High School in June, 1959.

The author attended Manhattan College from 1959 to 1963, receiving his Bachelor of Civil Engineering Degree in June, 1963. He then worked as a Research Assistant in the Structural Metals Division of Fritz Engineering Laboratory, Lehigh University, while working for the Master of Science Degree in Civil Engineering